# Novel Amino Acid-Based β-Phosphorylated Nitroxides for Probing Acidic pH in Biological Systems by EPR Spectroscopy

Chembiochem DOI: 10.1002/cbic.201600550

*Sophie Thétiot-Laurent, Gaëlle Gosset, Jean-Louis Clément, Mathieu Cassien, Anne Mercier, Didier Siri, Anouk Gaudel-Siri, Antal Rockenbauer,[‡] Marcel Culcasi,* and Sylvia Pietri*

Aix Marseille Univ, CNRS, ICR, Marseille, France

[‡] Research Centre for Natural Sciences of the Hungarian Academy of Sciences, Institute of Materials and Environmental Chemistry, and Budapest University of Technology and Economics, Hungary

*Corresponding author E-mail: marcel.culcasi@univ-amu.fr

*To whom correspondence should be addressed.

Phone: +33 (0)4-91-28-90-25. Fax: +33 (0)4-91-28-87-58

**Abstract**

There is increasing attraction of measuring pH in biological studies using nitroxides having pH-dependent electron paramagnetic resonance (EPR) spectra. Aiming to improve the spectral sensitivity, $\Delta a_X$, of these probes (i.e. the difference between limiting EPR hyperfine splittings (hfs) in their protonated and unprotonated forms), we present here a series of novel linear α-carboxy, α'-diethoxyphosphoryl nitroxides constructed on an amino acid core and featuring a (α or α')-C−H bond. In buffers the three main hfs ($a_N$, $a_H$ and $a_P$) of their X-band EPR spectra vary reversibly with pH and, when it is inferred from $a_P$ or $a_H$ titration curves, a 2−4-fold increase in sensitivity is achieved vs reference imidazoline or imidazolidine nitroxides. Lead crystallized carboxylate **10b** (p$K_a$ ≈ 3.6), which demonstrated low cytotoxicity and good resistance to bioreduction, was applied to probe the stomach acidity in rats. The results pave the way to a novel generation of highly sensitive EPR pH markers.

**Keywords**

Nitroxide; pH probe; $^{31}$P NMR; EPR; Bioreduction; Molecular dynamics; Stomach acidity.

## Introduction

In living organisms the pH value is a fundamental parameter whose thorough regulation is essential for maintaining the structure of proteins and physiological functions, e.g., by sustaining the active conformation of biologically active macromolecules.[1] Although normal extracellular and cytosolic acid-base homeostasis is associated with a pH range of 7.0−7.3, a local, substantially acidic intracellular pH ($pH_i$) occurs at pH 3−6 in certain cellular compartments such as the endoplasmic reticulum, the trans-Golgi complex or secretory vesicles, e.g., to allow cell internalization pathways (endosome-lysosome system).[2] Besides, abnormal low pHs are associated with cellular dysfunctions and pathologies such as ischemia, oxidative stress[3], apoptosis[4] or tumor size progression.[5]

As non-invasive alternatives to pH microelectrodes, optical and spectroscopic methods to assess pH in vivo have been the focus of intense research in the last decades. To sense $pH_i$ this usually involves introducing in tissue or cells weak acids displaying pH-dependent fluorescence (indicator dyes)[6,7] or $^{31}P$ NMR parameters (i.e., chemical shift and/or coupling constants).[6,8] Recently, structural modifications around the α- and β-aminophosphonate scaffold (cyclic or linear) have provided a series of non toxic pH markers showing finely tunable subcellular permeation and p$K_a$ value, with up to fourfold increased $^{31}P$ NMR sensitivity compared to endogenous inorganic phosphate ($P_i$).[9] Some of these compounds having a p$K_a$ < 6 were successfully applied to probe acidic compartments in isolated rat liver, amoeba cultures and plant cells (Figure 1A).[10]

The above spectroscopic techniques having their own limitations such as relative lack of sensitivity or requirement of nonabsorbing samples, interest in exogenous ionizable paramagnetic probes arose because much lower concentrations can be detected with short acquisition times using continuous wave X-band (~9.8 GHz) EPR spectroscopy. Up to now synthetic efforts have established imidazoline (Im)- and imidazolidine (In)-based nitroxides as the most utilized pH spin probes in biological studies, a model compound being 2,2,3,4,5,5-hexamethylimidazolidine-1-yloxy (In-1; Figure 1B).[6] These free radicals show low toxicity, rather good resistance to reduction into EPR-silent species, and substitution can be varied as to offer modulation of their lipophilicity, cell permeability and targeting.[11] In both Im

and In families protonation occurs at N-3, leading to a reversible variation of the two main apparent EPR parameters, the nitrogen hyperfine splitting (hfs) $a_N$ and *g*-factor. Furthermore, a wide range of p$K_a$s is accessible upon varying the electronic effects of substituents of the five-membered ring backbone.[12] Combining low-field (< 1.2 GHz) EPR techniques with appropriately tailored Im- or In-type pH reporters (i.e., with p$K_a$ < 5) allowed monitoring drug-induced changes in the gastric acidity of rats.[13]

Besides the necessary innocuity and stability conditions for a good EPR probe, high accuracy of pH measurement requires the largest sensitivity $\Delta a_X$ for a given coupling nucleus X to be achieved, where $\Delta a_X = |(a_X)_b - (a_X)_a|$ is the absolute difference of the coupling constants in the unprotonated basic and protonated acid forms of the radical. Since generally $a_{14\text{-}N} \approx 15$ G in nitroxides and the reported $\Delta a_N$ values in the Im and In families did not exceed 1.25 G so far[12a], our goal was to develop new ionizable β-phosphorylated nitroxides on the basis of their known large $a_P$ hfs, e.g., they are often > 40 G in the 1-pyrrolidinyloxyl series.[14,15] Despite this advantage of getting increased sensitivity only two studies have addressed EPR pH effects of such five membered ring nitroxides substituted by a β-P(O)$(OH)_2$ group, reporting total $a_P$ variations > 3 G in the whole pH range.[15] Yet none of these radicals (one of them being a spin adduct[15b]) were further evaluated in vivo and it is noteworthy that, because of the presence of two ionizable sites in the phosphono group, the useful $\Delta a_P$ value for a single acidity may be actually lower. Hence, for a total variation of 3.8 G in the biphasic titration curve of Ref.[15b], the useful $\Delta a_P$ is only ≈ 2 G around p$K_a$ 7.5. Such observation supports our earlier strategy in $^{31}$P NMR studies[9a] that a better sensitivity for spectral pH measurement is obtained when the ionizable site is remote to the NMR resonant (or EPR coupling) phosphorus.

With this concept in mind, our target EPR probes for acidic pH were α-carboxy, α'-diethoxyphosphoryl nitroxides where (i) ionization occurs at the $CO_2H$ function and (ii) the scaffold (Figure 1C) is close to that of linear α-aminophosphonates we developed as $^{31}$P NMR pH probes.[9] Many fully alkylated members of this family, such as *N*-*tert*-butyl-*N*-[1-diethylphosphono(2,2-

dimethylpropyl)] nitroxide (DEPN; Figure 1C), have become popular in nitroxide-mediated living polymerization[16] and more recently a small set of α-substituted acyl derivatives has been used to model solvent-related EPR hfs.[17] Although they bear one α-hydrogen, all these nitroxides are very persistent in solvents and water because their disproportionation into diamagnetic species can be prevented or slowered by steric crowding at the remaining α,α' positions[18], a substitution pattern we adopted in our target nitroxides by using (Y,Y') = Ph, *i*-Pr or *t*-Bu groups (Figure 1C). In this paper we report on our first foray into the EPR characteristics and biological in vitro activities of novel non-cyclic amino acid-based β-phosphorylated nitroxides. The lead isolable compound that emerged from this series was successfully applied to determine by X-band EPR the stomach acidity of living rats, in comparison with a structurally related α-aminoester especially developed for $^{31}$P NMR.

## Results and Discussion

**Synthesis.** All syntheses of target amino acid-derived β-diethoxyphosphoryl nitroxides proceeded via the formation of their α-aminophosphonate precursors, whose esters were isolated to evaluate their pH-dependent $^{31}$P NMR properties in comparison to other probes of the same class (Figure 1A).[9,10] The key step was a classical Kabachnik-Fields reaction with diethylphosphite and the appropriate carbonyl compound and α-amino acid, using either a one-pot procedure or a pathway where the intermediate imine was isolated. Desired nitroxides were derived by oxidation of α-aminophosphonates with *m*-chloroperoxybenzoic acid (*m*-CPBA). The syntheses of a series of α-aminophosphonates constructed from α-amino acids have already been described.[19]

The one-pot sequence was applied to diethylphosphite and acetone to derive the methyl esters **3a**−**c** of alanine, valine and phenylglycine, respectively, starting from the corresponding free amino acid esters **2a**−**c** (Scheme 1). Saponification of **3a**,**c** yielded the α'-diethoxyphosphoryl carboxylic acids **4a**,**c** in good yields. Intriguingly, attempts to hydrolyze **3b** by varying base, solvent, temperature and reaction time were unsuccessful. This appears consistent with the reported impossibility of saponifying alkyl

esters in α-position of an *i*-Pr substituent.[20] Finally, target nitroxides **5a**,**c** (for which Y' = Z' = Me; Figure 1C) were obtained by oxidation of **4a**,**c** with aqueous *m*-CPBA. Buffered solutions of **5a**,**c** were EPR stable for at least 3 h at ambient temperature.

**Scheme 1.** Synthesis of α-aminophosphonates **3a−c** and **4a,c** and nitroxides **5a**,**c**[a]

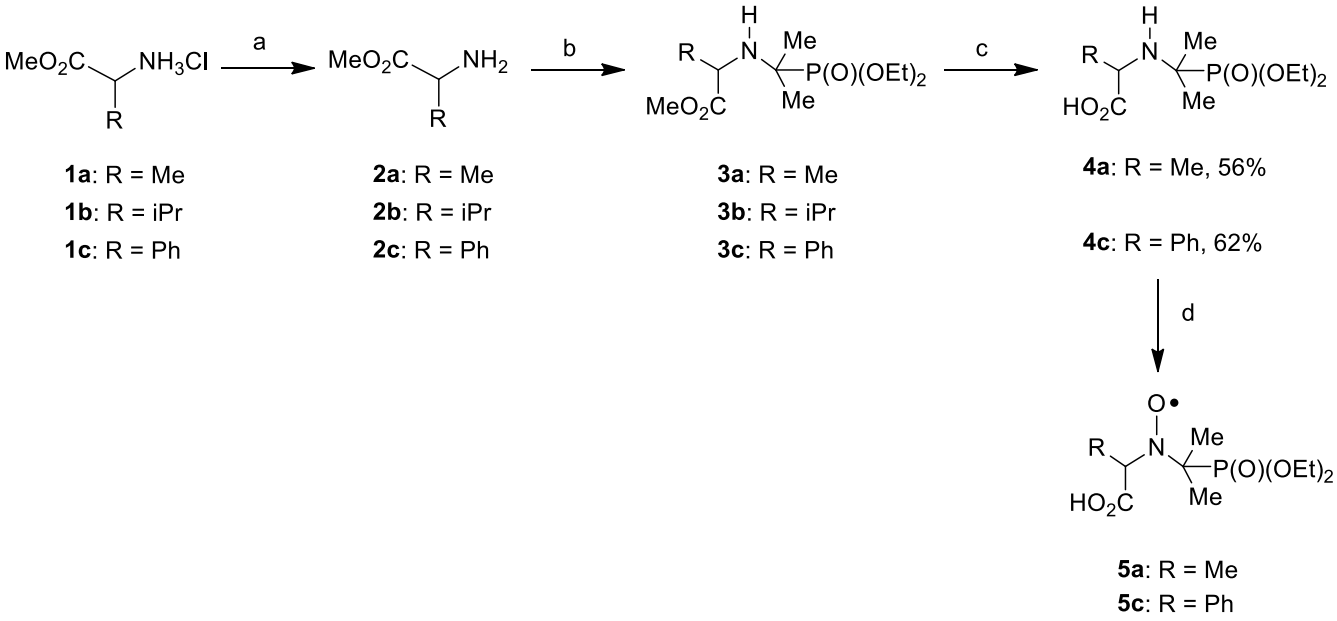


[a]Reagents and conditions: (a) ammonia, $Et_2O$, 4 h; (b) diethylphosphite, $Na_2SO_4$, acetone, reflux, 18 h, 54−60% over steps a+b; (c) 5 N NaOH, rt, then concentrated $H_2SO_4$; (d) *m*-CPBA, buffer pH 7.4 or cell homogenate, rt.

To synthesize target nitroxides for which Y = Z = Me, α,α-dimethylated amino acid based α'-diethoxyphosphoryl esters were prepared starting from 3-aminoisobutyric acid **6** which was esterified quantitatively to the ethyl ester hydrochloride **7**. Subsequent treatment of **7** by either pivaldehyde or isobutyraldehyde using a reported procedure[21] afforded the corresponding imines **8a**,**b** with good yields (Scheme 2). Microwave-assisted addition of diethylphosphite to **8a**,**b** gave the 2-aminoisobutyric acid-derived α-aminophosphonates ethyl esters **9a**,**b** in rather good yields. Oxidation of **9a**,**b** with *m*-CPBA using a slight modification of a reported procedure[16a] quantitatively yielded the corresponding esters nitroxides **10a** and **12** which were isolated as oils. Saponification of **10a** with NaOH gave the target

α,α-dimethylated β'-phosphorylated nitroxide (with an overall yield of 23% for the five steps), whose sodium salt **10b** afforded stable crystals. However, under the same base hydrolysis conditions the *i*-Pr analog **12** failed to give the expected nitroxide **11b** as checked by EPR.

**Scheme 2.** Synthesis of α-aminophosphonates **9a**,**b** and **11a** and related nitroxides **10a**,**b**, **11b** and **12**[a]

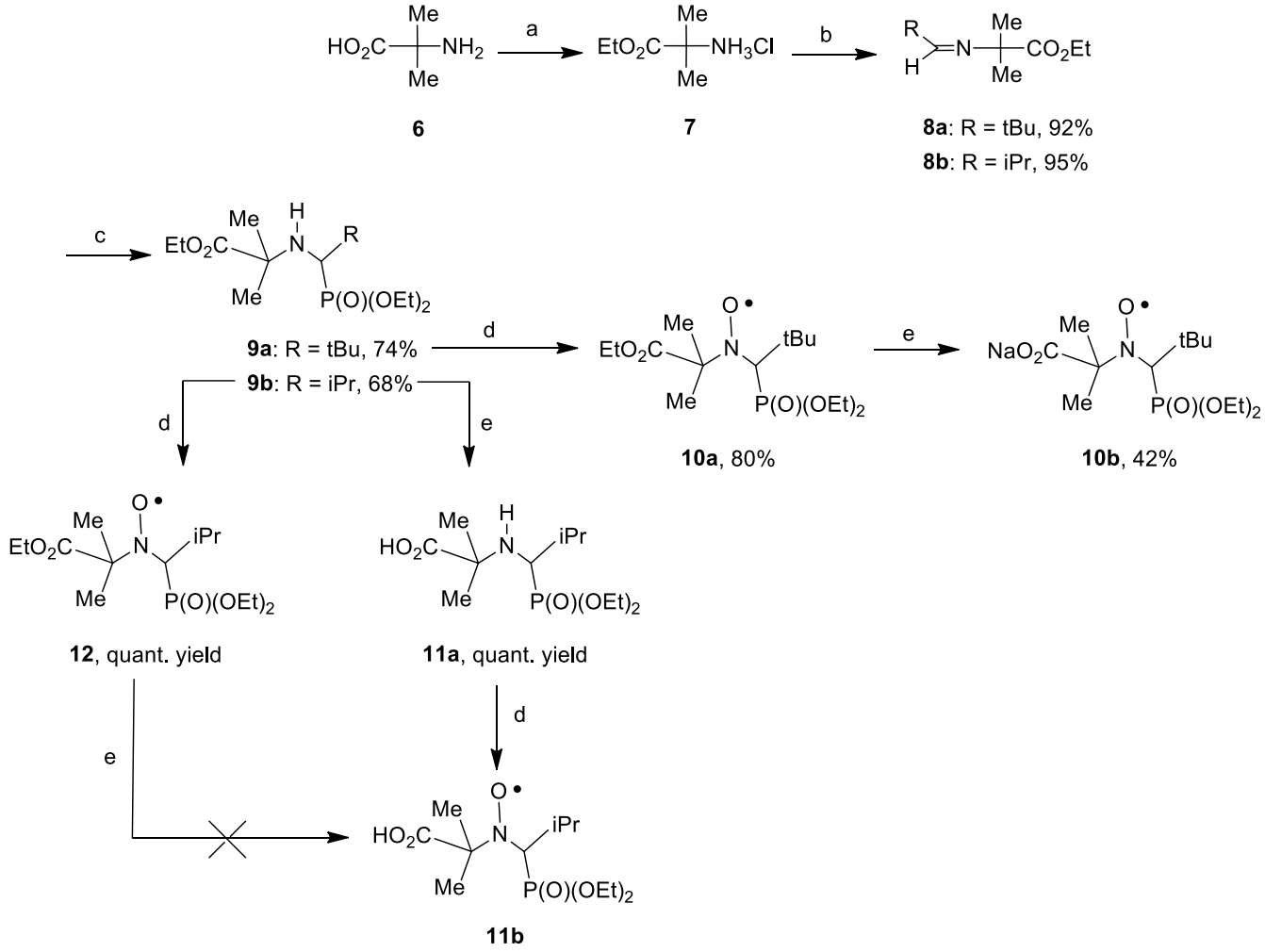


[a]Reagents and conditions: (a) $CH_3COCl$, EtOH, 85 °C, 12 h, quantitative yield; (b) pyvaldehyde (for synthesis of **8a**) or isobutyraldehyde (for synthesis of **8b**), $CH_2Cl_2$, TEA, 50 °C, 15 or 6 h, respectively; (c) diethylphosphite, microwaves, 150 °C, 45 min (synthesis of **9a**) or 30 min (synthesis of **9b**); (d) *m*-CPBA, $CHCl_3$ (synthesis of **10a** and **12**) or buffer pH 7.4 (formation of **11b**), 0 °C, then rt 2 h; (e) 5 N NaOH, rt, 15 h.

Nevertheless, nitroxide **11b** was obtained in two steps, i.e., saponification of **9b** to give the α-aminophosphonate α-carboxylic acid **11a** whose oxidation with aqueous *m*-CPBA gave **11b**. When prepared in situ such solutions of **11b** exhibited EPR stable signals for at least 3 h but again attempts to isolate the nitroxide by organic solvent extraction resulted in degradation, EPR silent products.

Lastly, we came to prepare α-aminophosphonate **16** (Scheme 3) to assess whether increasing both electron donating property and steric hindrance at α-C may affect the p$K_a$ value.

Commercially available (*S*)-methylvaline **13** was quantitatively converted to the ethyl ester hydrochloride **14**, whose subsequent reaction with pivaldehyde gave the corresponding imine **15** with a good yield. While microwave-assisted condensation of diethylphosphite on **15** only yielded degradation products, a 1:1 mixture of diastereomers of the desired compound **16** was obtained in moderate yield upon heating the imine at 55 °C for two weeks in a sealed tube.

After separation by chiral preparative HPLC (Chiralpak IC eluting with hexane/isopropanol/chloroform (8/1/1)), the stereochemistry of the two diastereomers was determined by NMR studies including $^1$H−$^1$H 2D ROESY experiments. For the first eluting diastereomer at $t_R$ = 4.87 min one ROE correlation was observed between the isopropylic proton ($\delta$ 1.82 ppm) and the α'-C−H (δ 2.73 ppm), demonstrating a (2*S*,1'*R*)-**16** configuration (Figure S1a, Supporting Information). For the second eluting diastereomer at $t_R$ = 6.05 min one ROE correlation was observed between the α'-C−H ($\delta$ 2.95 ppm) and the protons of the α-C−Me ($\delta$ 1.11 ppm), demonstrating (2*S*,1'*S*)-**16** configuration (Figure S1b, Supporting Information).

Subsequent oxidation by *m*-CPBA of (2*S*,1'*R*)-**16** and (2*S*,1'*S*)-**16** afforded the corresponding nitroxides (2*S*,1'*R*)-**17** and (2*S*,1'*S*)-**17** in good yields. Disappointingly, in relation to compound **3b** all diastereomeric α-*i*-Pr substituted esters **16** and **17** resisted hydrolysis (that should have yielded compounds **18** and **19**) and when drastic conditions (strong base, high temperature, long reaction time) were used, only decomposition products were recovered.

**Scheme 3.** Synthesis of diastereomeric α-aminophosphonates esters **16** and related nitroxides esters **17**[a]

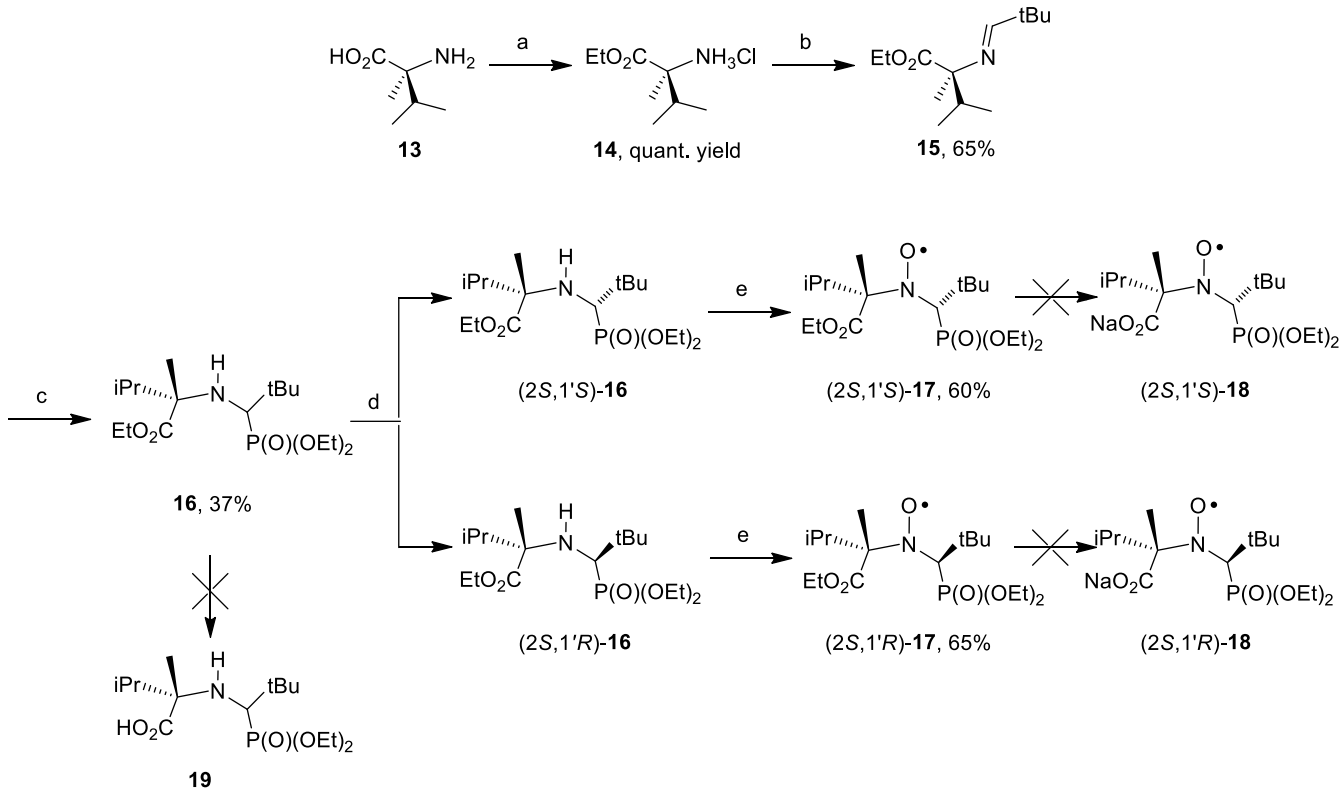


[a]Reagents and conditions: (a) $CH_3COCl$, EtOH, 85 °C, 12 h; (b) pivaldehyde, $CH_2Cl_2$, TEA, rt, 72 h; (c) diethylphosphite, 55 °C, 15 d; (d) Chiralpak IC, hexane/isopropanol/chloroform (8/1/1); (e) *m*-CPBA, $CHCl_3$, 0 °C, 4 h.

**$^{31}$P NMR pH-Calibration of α-Aminophosphonates Esters.** Besides the principal goal of this study, we investigated the pH dependence at 22 °C of the $^{31}$P NMR chemical shift of the new alkyl ester derivatives **3a**−**c** and **9a**,**b** in various physiologically relevant media, including Krebs-Henseleit buffer (KH) as well as KCl (125 mM)-supplemented cytosolic homogenates from rat heart ($CytM_h$) or liver ($CytM_l$).

All the esters, except diastereomers of **16**, gave monophasic acid-base titration curves reflecting protonation at nitrogen and their fitting to the Henderson-Hasselbalch equation (see Methods and Figure S2, Supporting Information) allowed calculation of the p$K_a$s, the limiting chemical shifts of the protonated ammonium ($\delta_a$) and unprotonated amine ($\delta_b$) forms, and the $^{31}$P NMR sensitivities $\Delta\delta_{ab}$ =

$\delta_a - \delta_b$ around the p$K_a$ region (Table 1). The five titrated compounds yielded acidic p$K_a$s ~3 with only < 2% variation with medium (i.e., ± 0.04−0.12 pH units). Owing to the strong electron withdrawing effect of ester groups, these quite low p$K_a$s for **3a**−**c** and **9a**,**b** confirm our previous findings[9,10] that, in β-diethoxyphosphoryl aminophosphonates, introducing inductive attractors (e.g., phenyl or benzyl) at $C_\alpha$ and/or $C_{\alpha'}$ results in more acidic p$K_a$ values (Figure 1A). Among our reported $^{31}$P NMR pH indicators, only a few cyclic (i.e., β-phosphorylated pyrrolidines) or linear (e.g., compound with $R_5$ = P(O)(OEt)$_2$ in Figure 1A) derivatives featuring two P-containing groups demonstrated p$K_a$ values < 3.5.[9a,10b]

Regarding the main characteristics of $^{31}$P chemical shift pH titration, compounds **3a**−**c** and **9a**,**b** showed very high $\Delta\delta_{ab}$ values of ~10 ppm with < 1% changes with medium (i.e., ± 0.15−0.73 ppm) and much shorter longitudinal relaxation times $T_1$ than the poorly sensible $P_i$.[22] Moreover, in KH the NMR sensitivities found for all tested esters were similar to that of DPP (i.e., ~10.2 ppm at 25 °C)[9c], a highly sensitive alkylated α-aminophosphonate pH sensor (Figure 1A) in the 5−8 pH range.[9a] In the case of diastereomers of **16** for which no sigmoidal acid-base curves could be obtained (i.e., $\Delta\delta_{ab} \approx 0$), longer $T_1$ values were yet measured at pH 4 (Table 1). In principle, the homogeneous low p$K_a$s found here for all aminophosphonates esters, giving a useful pH range of 1.5−4.5 with great NMR dynamic range, would encourage their use to probe subcellular acidic compartments or study physiological conditions such as gastric acidity.

**Crystal Structure of Nitroxide 10b and Molecular Dynamics Study.** The sodium carboxylate **10b** crystallizes as a dimer pooling two $Na^+$, with each cation being linked to six oxygen atoms (from two phosphonyl groups, the nitroxyl oxygen and carboxylate anion, and two water molecules), plus μ²-bridging performed by the two P=O functions and one water molecule. The structure appears similar to a square bipyramid centered on $Na^+$, the tops being occupied by a P=O group and a water molecule.

Chiral HPLC analysis revealed that the synthesis of **10b**, which is chiral at α'-C (Figure 1C), produced a racemate.

Figure 2A depicts an ORTEP view of one molecular unit of **10b** in the dimeric aggregate, in which (α,α')-C, P and β-H atoms surrounding the N-O• function are highlighted and where the α'-C retains a (*S*) configuration. The main X-ray crystallographic features of **10b**, i.e., elongated $C_{\alpha'}$−C(tBu), (α,α')-C−N and $C_{\alpha'}$−P bonds, and a large $C_{\alpha}$−N−$C_{\alpha'}$ bond angle (Table 2), result from the steric effect of the two bulky alkyl groups in α,α' positions. Similar geometries have been reported for the DEPN derivatives **20**[16a] and **21**[16b] (Figure 1, left panel) but unlike this latter nitroxide, the strongest stabilizing electrostatic interaction in crystallized **10b** is likely to establish between the partially positively charged N-atom and the carboxylate anionic oxygen rather than the phosphonyl oxygen[16b], as shown by the *d*(N...O) distance of 2.683 Å which is notably smaller than the NO van der Waals radii sum (~ 3.07 Å; see[16b] and references therein). Indeed the preferred electronic structures indicated in the headings of Table 2 for **10b** and related compounds account for the fact that in the unprotonated (basic) form of the radical the electron-donating effect of the $CO_2^-$ group will favor the resonance dipolar form (b) of the nitroxide function while the electron-withdrawing effect of the $CO_2H$ group in the protonated (acid) form will favor the non-polar form (a), as depicted in the right panel of Figure 1C.

To better understand the structural features responsible for the good stability in solution of acidic and basic forms of **10b** and its congeners **5a**,**c** and **11b** (see below and Methods), molecular dynamics (MD) simulations of the EPR spectra recorded at room temperature were performed to study the conformational changes of the solvated nitroxides (see Methods for details). Because the chirality of the probes (at either $C_{\alpha}$ or $C_{\alpha'}$) can in principle affect the distribution of the conformations, (*R*)/(*S*) enantiomers were considered (four trajectories for each compound). Table 2 reports the results of MD simulations for the (*S*) enantiomer of the nitroxides and results for the (*R*) enantiomer led to the same conclusions below (Table S1, Supporting Information). Comparing the angle and bond lengths pointed

out in the X-ray crystallographic structure of **10b** to computed values in solution revealed no or little variations suggesting that the β-H atom in all nitroxides remains sterically protected from disproportionation. Besides, none of the calculated *d*(N...O) distances in the unprotonated forms or *d*(COOH...O=P) and *d*(COOH...O−N) distances in the acidic forms (these being all > 3.8 Å, data not shown) were compatible with intramolecular bonds, e.g., H-bonds. Therefore the strong interaction found above for **10b** in the solid state likely results from a crystal packing effect.

**EPR Characterization.** To construct accurate EPR pH-titration curves for the novel ionizable nitroxides, high-resolution signals are needed in order to separatate the contributions of different species and to calculate the best sets of hfs at a given pH value. This was achieved by recording the spectra in deoxygenated buffer using low modulation amplitude, as illustrated by Figure 3A for **10b** at room temperature in phosphate buffer, pH ~7. The 12-lines EPR signals given by all carboxylic nitroxides and their ester precursors in aqueous solution clearly show that, in addition to $a_N$ and $a_P$ coupling constants observed in this class of radicals, the $a_{H\beta}$ hfs were also resolved. Moreover, simulation of the highly resolved spectrum of **10b** gave the best fit (r > 0.996) assuming a single species with additional long-range hfs with both α-C-Me groups and the *t*-Bu group, and a $^{13}C$ splitting pattern involving both α, α'- and the three β-carbons. Assuming the same long-range coupling model, the hfs and *g*-factors of the novel nitroxides at nearly neutral pH (except for **12**) were calculated (Table 3) and used as starting sets in EPR titration curves of ionizable compounds (which are all unprotonated under these conditions, see below). In the case of the EPR spectrum of DEPN in phosphate buffer, where only six lines can be resolved, we performed simulations including also β- and γ-hydrogen hfs besides the nitrogen and phosphorous couplings, which improved dramatically the fit (r > 0.996), yielding a reliable $a_{H\beta}$ value ~1 G, even though no further splitting occurred giving the expected 12 lines pattern.

According to the simplified Heller-McConnell relationship[23] the mean EPR β-couplings, $\langle a_X \rangle$ (X = H, P), of our target nitroxides in solution follow a dihedral dependence

$$\langle a_X \rangle = B_X \times \langle \cos^2\theta_X \rangle \qquad (1)$$

where $\theta_X$ is the dihedral angle between the N−C−X plane and the direction of the $2p_z$ orbital at nitrogen atom of the N−O• function (see Figure 2B in the case of **10b**). Accordingly, unlike DEPN, **20**, **21** and congeners which yield EPR sextets in organic solvents[16,17], all nitroxides of our series should adopt a preferred conformation in aqueous medium with a $\theta_H$ value not close to 90°, i.e., the N−O and $C_\alpha$−$H_\beta$ (for **5a**,**c**) or $C_{\alpha'}$−$H_\beta$ (for **10b** and **11b**) bonds are not totally eclipsing. This geometry was observed in the X-ray structure of **10b** since packing constraints the $H_\beta$−$C_{\alpha'}$−N−O and P−$C_{\alpha'}$−N−O torsion angles to about 171° and −76°, respectively (Table 2), corresponding to dihedral angles of $\theta_H \approx$ 99° and $\theta_P \approx$ 13° (Figure 2A). For both enantiomers of nitroxides **5a**,**c**, **10b** and **11b**, the average values of the torsion angles obtained from the MD simulation studies in water over the last 99.5 ns of the trajectory are reported (Tables 2 and S1). Conformational changes due to the release of crystal packing and minimization of steric constraints always tended to increase $H_\beta$−$C_{(\alpha,\alpha')}$−N−O dihedral angles in both basic and acidic forms near to 180° (corresponding to $\theta_H$ = 90°) with consequences on the EPR couplings as discussed below.

While establishing accurate sets of EPR hfs for all nitroxides we observed unusually intensive lines in the EPR signal of the ethyl ester (2*S*,1*R'*)-**17** in degassed water (not shown). A nice fit of the spectrum was obtained (r > 0.996) assuming a very large γ-hydrogen splitting of ~4 G, almost 2.7 times exceeding $a_{H\beta}$ (Table 3). We propose such a large long-range coupling in (2*S*,1'*R*)-**17**, but not in its diastereomer (2*S*,1'*S*)-**17**, to result from a periplanar 'W-plan' arrangement, as reported earlier in *i*-Pr-substituted cyclic nitroxides.[24]

**EPR pH Titration.** In eq 1 the experimentally determined hyperconjugative parameters $B_H$ and $B_P$ in β-phosphorylated nitroxides are of 26 G and 58 G, respectively.[14,25] We thus reasoned that in our novel ionizable stable nitroxides, even a minute pH-induced conformational change, leading to $\theta_H$ and/or $\theta_P$

variation, would translate to large $\Delta a_H$ and/or $\Delta a_P$ values, the latter being potentially larger due to the greater $B_P$ constant. Indeed pH-dependent EPR spectra were obtained with the four carboxylic nitroxides **5a**,**c**, **10b** and **11b** (illustrated in Figure 3B for **10b** and **5c)** while non ionizable esters **10a**, **12** and **17** exhibited pH-insensitive EPR signals. With parameters of Table 3 as starting points of the simulations a set of three monophasic EPR pH titration curves involving $a_N$, $a_H$ and $a_P$ hfs were obtained for each carboxylic nitroxide in 20 mM phosphate buffer or cytosolic homogenates at 22 °C. Titration curves for **10b** and **5a,c** are shown in Figures 4 and S3 (Supporting Information), respectively. Importantly, these plots were obtained by reversibly sweeping a 0.5−12 pH window for about 1.5 h without any noticeable loss of EPR signal.

Table 4 reports the limiting hfs and p$K_a$s obtained either by fitting the pH titration profiles (each spectrum was simulated individually) to the EPR variant of the Henderson-Hasselbalch eq 3 (Supporting Information) or by a two-dimensional (2-D) procedure[26] involving simultaneous fitting of the whole set of parameters (hfs, *g*-value, linewidth and p$K_a$) for each titration. Regardless of the nucleus considered, limiting hfs and p$K_a$s of **5a**,**c** and **10b** in synthetic buffer vs the various CytM prepared from rat organs were not substantially altered, varying by less than 0.1 G and 0.2 pH units, respectively. In particular $a_N$ values remained almost constant although spin density at nitrogen in β-phosphorylated nitroxides is known to increase with solvent polarity.[15a,17] For all nitroxides in a given milieu, acidic p$K_a$s extracted from the three $a_X$ (X = N, H, P) vs pH titration curves ($n$ = 2−4) showed little variation (≤ 0.06 pH units), except when $a_H$ was used to probe pH using **11b**, probably because of the very small EPR sensitivity found in this case. As compared with these data, 2-D calculation yielded small differences in limiting hfs (< 0.2 G; not shown) but slightly different p$K_a$s which however followed the same trend among compounds (Table 4). In agreement with the known effect of electron-withdrawing substituents in α-position of the carboxylic acid function, the lowest p$K_a$ in the nitroxide series found for **5c** vs **5a** follows the trends observed for **3c** vs **3a** in the $^{31}$P NMR study (Table 1) and of the α-amino acids building blocks phenylglycine vs alanine, which show p$K_a$s of 1.83 vs 2.34,

respectively. In another hand, protonation/deprotonation of the nitroxides generates a characteristic linewidth alternation responsible for slightly asymmetric EPR lines as seen in Figure 3. The proton exchange times calculated by 2-D simulation were 13.2, 13.8, 104 and 31 ns for **5a**,**c**, **10b** and **11b**, respectively, reflecting a fast exchange on the EPR time scale.

As anticipated, an important feature of novel nitroxides pH markers is their enhanced EPR sensitivity in the acidic region making them good candidates to probe the gastric pH in vivo. Consistent with the high potential of conformational-related variation of hfs, **5a**,**c** offered the best properties, e.g., for **5a**: $\Delta a_H$ = 2.35 G and $\Delta a_P \approx$ 3.7 G while **10b** still showed appreciable interest, with $\Delta a_P \approx$ 1.9 G (Table 4). It is worth underlining that unlike our lead compound **10b**, related nitroxides having demonstrated $\Delta a_P$ values up to 3.5 G were not isolated.[15]

In the Im-(1,2) and In-(1,2) families developed as EPR pH probes (Figure 1B) a through-bond mechanism operates by which protonation/deprotonation modifies spin density at nitrogen, and thereby pH sensing mainly relies on changes in $a_N$.[6,11,12] In our designed nitroxides a deprotonation-induced rise in $a_N$ occurred as the resonance form (b) becomes predominant (Figure 1C, left panel) with $\Delta a_N$ values ranging 0.18−0.38 G (Table 4), yet below the sensitivities of In-1 nitroxides having acidic p$K_a$s.[12,13a]

In **10b** and **11b**, the finding that $a_H$ increases (that is, $\theta_H$ decreases) while $a_P$ decreases (that is, $\theta_P$ increases) upon increasing pH (Figure 4 and Table 4) is an obvious consequence of eq 1 (schematized in Figure 2B) since in these nitroxides the coupling nuclei H and P are attached to the same $C_\alpha$'. In **5a**,**c** where H and P are linked to $C_\alpha$ and $C_\alpha$', respectively, both $a_H$ and $a_P$ increased with pH (Figure S3 and Table 4). These opposite trends were confirmed by applying eq 1 with $B_P$ = 58 G to $\theta_P$ angles derived from MD simulations of P−$C_\alpha$'−N−O dihedral angle in the protonated and unprotonated forms of the nitroxides (Tables 4 and S1). Assuming a (*R*)/(*S*) racemic mixture for **5a**,**c**, **10b** and **11b** gave predicted absolute $\Delta(\langle a_P \rangle)$ values of 2.1, 4.1, −0.6 and −2.8 G, respectively, in relatively good agreement (especially the sign was well reproduced) with the corresponding experimental values of 3.74, 3.88,

−1.87 and −0.36 G, respectively (Table 4). For **5a**,**c** dihedral angle distributions revealed two symmetric positions in the protonated forms while the $P(O)(OEt)_2$ moiety adopts almost the same orientation in the unprotonated form (Figures S4 and S5, Supporting Information). For (**10b**, **11b**) no significant changes in dihedral distributions with pH were found (Figures S6 and S7, Supporting Information) suggesting that phosphoryl group rotation is almost frozen. Altogether these data could explain the differences (amplitude and sign) of $\Delta<a_P>$ between the two couples of nitroxides. In accordance, MD simulation of $H_\beta-C_{\alpha'}-N-O$ dihedral angle predicts smaller standard-deviation values for (**10b**, **11b**) vs **5a**,**c** (Table 2) in agreement with larger experimental $\Delta a_{H\beta}$ values in these latter nitroxides (Table 4).

**Bioreduction Studies.** In vivo, nitroxides are converted to diamagnetic hydroxylamines by antioxidants such as ascorbate and glutathione, or by enzymatic systems located, e.g., in liver microsomes. To assess the metabolic stability of **10b** near its p$K_a$ it was incubated at 37 °C in the presence of $CytM_l$ in phosphate-citrate buffer adjusted to pH 3.5 and compared to non ionizable β-phosphorylated nitroxide 2-diethoxyphosphoryl-2,5,5-trimethylpyrrolidine 1-oxyl (TMPPO) and the widely studied 3-carboxy-2,2,5,5-tetramethylpyrrolidine 1-oxyl (3-CP) which demonstrates an acidic p$K_a$ = 4.0 but a weak EPR pH reporting property ($\Delta a_N$ = 0.19 G).[27] At pH 3.5 the rates of reduction and half-lifes, determined under pseudo first-order conditions from the relative decay curves of **10b**, 3-CP and TMPPO (Figure 5), were $k_{red}$ = 0.27 ± 0.03, 0.29 ± 0.02 and 0.07 ± 0.02 $min^{-1}$ and $t_{1/2}$ = 3.1, 2.5 and 14.5 min, respectively, indicating that both carboxylic nitroxides are reduced at a significantly faster rate. When incubations were carried out in KH adjusted to pH 7.0, **10b** became the more resistant compound, with kinetic parameters ranking: $k_{red}$ = 0.10 ± 0.01, 0.16 ± 0.02 and 0.29 ± 0.04 $min^{-1}$ and $t_{1/2}$ = 9.5, 4.3 and 2.4 min for **10b**, 3-CP and TMPPO, respectively. Such difference in stability with pH is not unexpected since the reduction of the carboxylate form, which is the dominant species at neutral pH for **10b** and 3-CP, is clearly unlikely.[28] Abundant literature addressing structure-activity relationships for the stability toward reductants of cyclic nitroxides, including Im and In classes of EPR pH markers,

has identified α,α'-tretraalkyl substitution of the ring as a key feature to sterically protect nitroxide function.[11c,28,29] In this regard **10b** appears an exception to this rule and it may have some interest in probing acidic cell compartments.

**In Vitro Toxicity Studies.** Cytotoxicity assays were performed on **10b** and selected α-aminophosphonates esters to investigate their effects on cell viability and metabolic activity in vitro. $IC_{50}$ values against human normal fibroblasts (NHLF) and lung cancer (A549) cell lines were determined by measuring the release of total intracellular lactate dehydrogenase (LDH) and by FMCA and MTT assays[30] following a 48 h incubation at 37 °C with test compounds (0.1−50 mM). The results are summarized in Table 5 along with that of reference compounds and calculated lipophilicities. In general all novel compounds, TMPPO and DEPN demonstrated low cytotoxicity, with $IC_{50}$ values in the millimolar range in the three assays, and in most cases A549 cells were found less sensitive than NHLF.

Nitroxides are being increasingly employed for their antioxidant properties, with the purpose of therapeutic use. Thus, we have reported on cardioprotective effects of low concentrations of TMPPO in ischemic rat hearts, with EPR signal of the nitroxide being still detected up to 30 min following reperfusion both in perfusate and tissue homogenate medium.[31] In order to ensure that negligible nitroxide degradation into secondary species susceptible to interfere with the assay may have occurred in cell medium when incubation time was prolonged, A549 cells were exposed to 15 mM of **10b**, TMPPO or DEPN for 48 h at 37 °C and no significant loss of EPR signals was found (not shown).

Among the tested compounds the most hydrophilic diethyl(2-methylpyrrolidin-2-yl) phosphonate (DEPMPH), a cyclic $^{31}P$ NMR pH marker already applied ex vivo[10a], yielded the highest $IC_{50}$ value. In contrast **3c** has increased cytotoxicity, a result that could account for its high lipophilicity and/or the presence of an aromatic substituent, as previously found in structural analogs such as those shown in Figure 1A.[9b] Based on their toxicity data and in view of obtaining well-resolved signals with short acquisition times, the concentrations of 3 and 5 mM for **10b** and **3a**, respectively, were selected for the next ex vivo spectroscopic experiments.

**In Vivo pH Measurement in the Rat Stomach.** According to the steepest part of their titration curves (Figures 4 and S2) and their p$K_a$ ≈ 3.6, **10b** and **3a** are appropriate to probe a ~2.1−5.1 pH window, which conforms to the admitted useful range of p$K_a$ ± 1.5 pH units for spectroscopic pH markers.[6] When anesthetized rats had their stomach filled for 30 min with a solution of **10b** (3 mM) in either phosphate buffer (5 mM; starting pH 7.19), or in bicarbonate (0.1 M; starting pH 8.41) or Maalox taken as antacids (starting pH 8.72), pH-dependent EPR spectra were obtained in gastric fluid samples. These signals, recorded at 22 °C five min after sampling, were strong enough to obtain good resolution (e.g., modulation amplitude < 0.1 G was applied) and a short sweep time (< 1.5 min), as can be seen in Figure 6A where only the four low-field doublets are shown to best visualize the changes in hfs. In normal gastric fluid, pH ~ 2.6, the EPR signal of **10b** exhibited a slower first-order decay ($k \approx 0.04$ min$^{-1}$ and $t_{1/2} \approx 20$ min) compared to the bioreduction process in $CytM_l$, with no change in hfs. In the rat stomach a better in vivo stability has been reported for two Im-type EPR pH probes, which yet show a 2-times lower spectral sensitivity vs **10b**.[13b]

Finally, a very good agreement was found between pH values determined spectroscopically and that obtained using a microelectrode (Figure 6B). We found differences ≤ 0.15 pH units among the three methods for a given condition when pH was obtained against the $a_P$ EPR titration curve in $CytM_s$ but alternate use of $a_N$ and $a_H$ hfs resulted in identical precision. Comparing EPR to $^{31}$P NMR, it should be noted that while the amine **3a** was very stable in the stomach fluid (typical $^{31}$P NMR spectra are shown in Figure S8, Supporting Information), a longer acquisition time was necessary (at least 8 min) to achieve a similar accuracy in pH determination. A sampling time of 30 min was selected in all groups on the basis of reported almost full normalization of gastric pH level in rats given an EPR pH probe with p$K_a$ ~4.9.[13b] In this time frame, the pH of the stock solutions of **10b** and **3a** stored at 37 °C remained neutral or slightly basic, stabilizing at less than +0.15 pH units vs the corresponding starting value. Therefore Figure 6B demonstrates in particular that **10b** (i) did not chemically interact with the early (5 min) relaxation of stomach pH, and (ii) faithfully probed the expected slower pH decrease in the

high-buffering capacity antacids vs phosphate buffer, in line with other EPR studies.[13] Thus, 30 min after administration of **10b** in 5 mM phosphate buffer, a physiologically relevant value for gastric pH of 2.58 ± 0.11 ($n$ = 7) could be determined.

## Conclusion

In our continuous efforts to discover a novel generation of spectroscopic pH markers, we have designed a series of α-hydrogen substituted, β-phosphorylated linear nitroxides based on an amino acid core structure. Notably, crystallized sodium carboxylate **10b** displayed triple sensing (using $a_N$, $a_P$ or $a_H$ couplings), pH dependent EPR spectra and its p$K_a$ = 3.6 and good resistance to bioreduction render it particularly suited to probe acidic sub-cellular compartments or study normal and pathological conditions linked to low pH. Based on known rules for EPR conformation-dependent hfs of β-substituted nitroxides, introducing a non-titrating phosphorus moiety in **10b** improved its spectral sensitivity by ~2-fold, as compared to the more rigid cyclic probes described before. Interestingly, even better sensitivities were obtained for **5a**,**c**, the isolation of which is in due course.

On the EPR side of this study, further follow-up will include a MD-assisted structure-based rational nitroxide design, with the general structure shown in Figure 1C as a starting point. In the course of the syntheses, a series of novel α-aminophosphonates esters were produced and their $^{31}$P NMR constants will increment our existing library of about 50 analog pH probes with the purpose of optimizing structure-activity relationships.

## Experimental Section

**Chemistry. General Methods.** All solvents and chemicals were reagent grade from commercial suppliers and were used as such. Doubly distilled deionized water was used throughout and test solutions were filtered through a 0.2-μm Millipore filter prior to use. Ultrapure DEPMPH[32] and diethyl(2-propylaminoprop-2-yl)phosphonate (DPP)[9a] were obtained as previously described. 3-CP was

from Sigma-Aldrich Chimie (St. Quentin Fallavier, France) and TMPPO was synthesized and purified as described.[29a] DEPN[16a] was a kind gift of Dr. D. Gigmes. Microwave reactions were conducted in an Anton Paar Monowave 300 reactor. Reactions were followed by TLC on Merck-Kieselgel 60 F254 precoated silica gel plates and the spots were visualized under UV light, or by staining with phosphomolybdic acid. Melting points were obtained using a Büchi Melting Point B-540 apparatus and are not corrected. Analytical NMR spectra were recorded using a Bruker Avance III Nanobay spectrometer. Chemical shifts ($\delta$) are reported in parts per million (ppm) relative to internal $Me_4Si$ ($^1H$ and $^{13}C$) or 85% external $H_3PO_4$ ($^{31}P$) and coupling constants ($J$) are given in hertz (Hz). Splitting patterns are reported as follows: s = singlet; d = doublet; dd = doublet of doublets; t = triplet; quint = quintuplet; hept = heptuplet; m = multiplet; br = broad peak. High-resolution mass spectrometry (HRMS) in electron spray ionization (ESI; Q-STAR Elite instrument, Applied Biosystems, USA) and elemental analyses (Thermo Finnigan EA 1112 series Flash elemental analyzer) were undertaken at the Spectropole (Analytical Laboratory) at Campus St. Jérôme (Marseille, France). Optical rotations were determined on an Anton Paar MCP200 polarimeter with a 0.2 cm length. The purity of all synthesized compounds was > 96% as ascertained by elemental analysis.

**Synthesis of Methyl Esters of Amino Acid Based Phosphonates 3a−c by the Kabachnik−Fields Reaction.** Dry ammonia was bubbled for 4 h into a suspension of the (*S*)-amino acid methyl ester hydrochloride **1a−c** in dry $Et_2O$ (60 mL). After filtration, $Et_2O$ was removed under reduced pressure and the resulting free amino acid methyl ester **2a−c** was processed without further purification as follows: a stirred mixture of diethylphosphite, **2a−c** and $Na_2SO_4$ (5.0 g, 35.2 mmol) was refluxed in acetone (30 mL) for 18 h. The mixture was filtered, concentrated in vacuum and the residue was purified to give the desired compound **3a−c** as detailed below.

*Methyl 2-{[2-(diethoxyphosphoryl)propan-2-yl]-amino}propanoate (**3a**).* Free alanine methyl ester **2a** was obtained as a colorless oil (4.6 g, 89%) from hydrochloride **1a** (7.0 g, 50.1 mmol). Compound **3a** was then obtained from **2a** (4.6 g, 44 mmol) and diethylphosphite (6.1 g, 44 mmol) according to the

above procedure. Distillation of the residue under reduced pressure afforded **3a** as a light yellow oil (7.4 g, 59%): bp 80 °C ($3.7 \times 10^{-2}$ mmHg); $^{1}$H NMR (300 MHz, $CDCl_3$) $\delta$ 4.15−4.12 (m, 4H, 2 × $CH_2$), 3.78 (quint, 1H, $J$ = 9.0 Hz, C*H*$CO_2$Me), 3.65 (s, 3H, $CO_2CH_3$), 1.89 (br s, 1H, NH), 1.29−1.18 (m, 15H, 5 × $CH_3$); $^{13}$C NMR (75.5 MHz, CDCl3) $\delta$ 177.5 (C=O), 62.5 (d, $J_{CP}$ = 7.5 Hz, $CH_2$), 62.0 (d, $J_{CP}$ = 7.5 Hz, $CH_2$), 53.1 (d, $J_{CP}$ = 153.2 Hz, C), 51.8 ($CO_2CH_3$), 51.0 (d, $J_{CP}$ = 4.5 Hz, CH), 23.9 (d, $J_{CP}$ = 3.8 Hz, C$CH_3$), 22.6 (d, $J$ = 3.8 Hz, C$CH_3$), 21.7 (CH$CH_3$), 16.5 (d, $J_{CP}$ = 3.0 Hz, $CH_2CH_3$), 16.4 (d, $J_{CP}$ = 3.0 Hz, $CH_2CH_3$); $^{31}$P NMR (121.5 MHz, $CDCl_3$) $\delta$ 28.9. Anal. Calcd. for $C_{11}H_{24}NO_5P$: C, 46.97; H, 8.60; N, 4.98. Found: C, 46.63; H, 8.60; N, 4.77.

*Methyl 2-{[2-(diethoxyphosphoryl)propan-2-yl]-amino}-3-methylbutanoate (**3b**)*. Free valine methyl ester **2b** was obtained as a colorless oil (4.6 g, 98%) from hydrochloride **1b** (8.9 g, 35.0 mmol). Compound **3b** was then obtained from **2b** (4.6 g, 37.3 mmol) and diethylphosphite (5.2 g, 37.3 mmol) according to the above procedure. The residue was purified by silica gel column chromatography eluting with pentane/acetone/methanol (80/18/2) to afford **3b** as a yellow oil (5.9 g; 54%). $^{1}$H (300 MHz, $CDCl_3$) $\delta$ 4.20−4.00 (m, 4H, 2 × $CH_2$), 3.70 (s, 3H, $CO_2CH_3$), 3.37 (d, 1H, $J$ = 6.0 Hz, C*H*$CO_2$Me), 1.94 (s, 1H, NH), 1.81 (m, 1H, C*H*$(CH_3)_2$), 1.33 (t, 3H, $J$ = 7.1 Hz, $OCH_2CH_3$), 1.32 (t, 3H, $J$ = 7.5 Hz, $OCH_2CH_3$), 1.25 (d, 3H, $J_{HP}$ = 11.0 Hz, $CCH_3$), 1.23 (d, 3H, $J_{HP}$ = 13.1 Hz, $CCH_3$), 0.91 (d, 3H, $J$ = 6.8 Hz, CH$(CH_3)_2$), 0.89 (d, 3H, $J$ = 6.8 Hz, CH$(CH_3)_2$); $^{13}$C NMR (75.5 MHz, $CDCl_3$) $\delta$ 176.6 (C=O), 62.3 ($CH_2$), 60.5 (NHCH), 53.3 (d, $J_{HP}$ = 158.2 Hz, C), 51.6 ($CO_2CH_3$), 32.9 (*C*H$(CH_3)_2$), 23.4 (2 × C$CH_3$), 19.4 (CH$(CH_3)_2$), 18.4 (CH$(CH_3)_2$), 16.7 (2 × $CH_2CH_3$); $^{31}$P NMR (121.4 MHz, $CDCl_3$) $\delta$ 30.4. Anal. Calcd. for $C_{13}H_{28}NO_5P$: C, 50.48; H, 9.12; N, 4.53. Found: C, 49.98; H, 9.39; N, 4.49.

*Methyl 2-{[2-(diethoxyphosphoryl)propan-2-yl]-amino}-3-methylbutanoate (**3c**).* Free phenylglycine methyl ester **2c** was obtained as a colorless oil (3.0 g, 92%) from hydrochloride **1c** (4.0 g, 19.8 mmol). Compound **3c** was then obtained from **2c** (3.0 g, 18.2 mmol) and diethylphosphite (5.0 g, 20.2 mmol) according to the above procedure. The residue was purified by silica gel column chromatography eluting with pentane/acetone (70/50) to afford **3c** as a light yellow oil (3.77 g; 60%). $^{1}$H NMR (300

MHz, $CDCl_3$) $\delta$ 7.43−7.41 (m, 2H, $H_{meta}$), 7.32−7.24 (m, 3H, $H_{ortho}$ and $H_{para}$), 4.99 (s, 1H, CH), 4.14−4.02 (m, 4H, 2 × $CH_2$), 3.66 (s, 3H, $CO_2CH_3$), 2.51 (br s, 1H, NH), 1.34−1.18 (m, 12H, $C(CH_3)_2$ and 2 × –$OCH_2CH_3$); $^{13}$C NMR (75.5 MHz, $CDCl_3$) $\delta$ 174.6 (C=O), 140.7 (Ar, Ph), 128.4 (Ar, Ph), 127.5 (Ar, Ph), 127.4 (Ar, Ph), 62.3 (d, $J_{CP}$ = 7.5 Hz, $CH_2$), 62.1 (d, $J_{CP}$ = 7.5 Hz, $CH_2$), 59.6 (d, $J_{CP}$ = 3.8 Hz, CH), 54.4 (d, $J_{CP}$ = 149.4 Hz, C), 52.3 ($CO_2CH_3$), 23.9 (d, $J_{CP}$ = 3.0 Hz, $CCH_3$), 23.4 (d, $J_{CP}$ = 3.8 Hz, $CCH_3$), 16.5 (d, $J_{CP}$ = 2.3 Hz, $CH_2CH_3$), 16.4 (d, $J_{CP}$ = 2.3 Hz, $CH_2CH_3$); $^{31}$P NMR (121.4 MHz, $CDCl_3$) $\delta$ 30.1. Anal. Calcd. for $C_{16}H_{26}NO_5P$: C, 55.97; H, 7.63; N, 4.08. Found: C, 55.69; H, 7.77; N, 4.01.

**Synthesis of Amino Acid Based Phosphonates 4a**,**c.** The appropriate compound **3a**,**c** (1.07 mmol) was stirred in aqueous NaOH (5 N, 3 mL) at rt until complete solubilization. The mixture was carefully acidified with $H_2SO_4$ to pH 1 and the aqueous phase was extracted with $Et_2O$ (3 × 5 mL). Combined organic layers were dried over $MgSO_4$, filtered and concentrated in vacuum to give the corresponding **4a**,**c** which were used without further purification.

*2-{[2-(Diethoxyphosphoryl)propan-2-yl]-amino}propanoic acid (**4a**).* Saponification of **3a** (0.3 g, 1.07 mmol) afforded **4a** as a yellow oil (0.16 g, 56%). $^1$H (300 MHz, $CDCl_3$) $\delta$ 5.36 (br s, 1H, NH), 4.17−4.06 (m, 4H, 2 × $CH_2$), 3.71 (quint, 1H, $J$ = 9 Hz, $CHCO_2H$), 1.34−1.24 (m, 15H, 5 × $CH_3$); $^{13}$C NMR (75.5 MHz, $CDCl_3$) $\delta$ 176.7 (C=O), 62.9 (d, $J_{CP}$ = 7.5 Hz, $CH_2$), 62.7 (d, $J_{CP}$ = 7.5 Hz, $CH_2$), 53.2 (d, $J_{CP}$ = 153.0 Hz, C), 51.4 (d, $J_{CP}$ = 3.8 Hz, CH), 23.2 (d, $J_{CP}$ = 1.5 Hz, $CCH_3$), 22.0 (d, $J_{CP}$ = 2.3 Hz, $CCH_3$), 20.3 ($CHCH_3$), 16.4 (d, $J_{CP}$ = 1.5Hz, $CH_2CH_3$), 16.3 (d, $J_{CP}$ = 1.5 Hz, $CH_2CH_3$); $^{31}$P NMR (121.4 MHz, $CDCl_3$) $\delta$ 29.72. Anal. Calcd. for $C_{11}H_{24}NO_5P$: C, 46.97; H, 8.60; N, 4.98. Found: C, 46.75; H, 8.70; N, 4.99.

*2-{[2-(Diethoxyphosphoryl)propan-2-yl]-amino}-2-phenyl-ethanoic acid (**4c**).* Saponification of **3c** (0.2 g, 0.58 mmol) afforded **4c** as a yellow oil (0.12 g, 62%). $^1$H (300 MHz, $CDCl_3$) $\delta$ 7.43−7.41 (m, 2H), 7.34−7.24 (m, 3H), 5.67 (br s, 2H, NH and $CO_2H$), 4.90 (s, 1H, CH), 4.17−4.04 (m, 4H, 2 × $CH_2$), 1.36−1.18 (m, 12H, 4 × $CH_3$); $^{13}$C NMR (75.47 MHz, $CDCl_3$) $\delta$ 174.4 (C=O), 139.9 (Ar, Ph), 128.6

(Ar, Ph), 127.9 (Ar, Ph), 127.4 (Ar, Ph), 62.8 (d, $J_{CP}$ = 3.0 Hz, $CH_2$), 62.7 (d, $J_{CP}$ = 2.3 Hz, $CH_2$), 59.9 (d, $J_{CP}$ = 3.8 Hz, CH), 53.4 (d, $J_{CP}$ = 150.9 Hz, C), 23.2 (d, $J_{CP}$ = 3.8 Hz, $CCH_3$), 23.1 (d, $J_{CP}$ = 3.0 Hz, $CCH_3$), 16.4 (d, $J_{CP}$ = 1.5 Hz, $CH_2CH_3$), 16.3 (d, $J_{CP}$ = 1.5 Hz, $CH_2CH_3$); $^{31}$P NMR (121.4 MHz, $CDCl_3$) $\delta$ 29.7. Anal. Calcd. for $C_{16}H_{26}NO_5P$: C, 55.97; H, 7.63; N, 4.08. Found: C, 55.53; H, 7.80; N, 4.09.

**In Situ Formation of Carboxylic Nitroxides 5a and 5c.** Solutions of the appropriate amine **4a**,**c** (100 mM) and a solution of *m*-CPBA (10 mM) were first prepared in phosphate buffer (i.e., 20 mM $KH_2PO_4$, pH 7.4). An aliquot of NaOH (1 N) was added to the *m*-CPBA solution (final concentration, 15%) to achieve complete solubilization of the peracid. Two hundred microliters of each solution of **4a**,**c** were then diluted to 10 mM by adding phosphate buffer or $CytM_h$[10a,31] (see preparation below), and an aliquot (30 μL) of *m*-CPBA solution was added to this mixture (final peracid concentration, 0.15 mM) to reach a final volume of 2 mL. The resulting working solutions of nitroxides **5a**,**c** can be used in EPR titration experiments within 3−4 h following addition of the oxidant.

**Synthesis of Aminophosphonates Esters 9a and 9b.** *Ethyl 2-amino-2-methylpropanoate hydrochloride (7)*. To a solution of 3-aminoisobutyric acid **6** (1.2 g, 11.72 mmol) in ethanol (50 mL) was added acetyl chloride (2.7 mL, 37.4 mmol, 3.2 equiv) at 0 °C under argon atmosphere. The resulting mixture was stirred at 85 °C for 24 h, cooled to rt and concentrated under reduced pressure to give **7** as a white powder (1.93 g, 11.5 mmol, quantitative yield); mp 155.7−155.9 °C (lit.[33] mp 156−157 °C). $^1$H NMR (300 MHz, $D_2O$) $\delta$ 4.18 (q, 2H, $J$ = 7.2 Hz, $CH_2$), 1.49 (s, 6H, $C(CH_3)_2$), 1.19 (t, 3H, $J$ = 7.2 Hz, $CH_2CH_3$); $^{13}$C NMR (75.5 MHz, $CDCl_3$) $\delta$ 172.5 (C=O), 63.7 ($CO_2CH_2$), 56.8 ($C(CH_3)_2$), 22.9 ($C(CH_3)_2$), 13.1 ($CO_2CH_2CH_3$).

*Methyl 2-{[1-(diethoxyphosphoryl)-2,2-dimethylpropan-1-yl]-amino}-2-methylpropanoate (**9a**)*. To a solution of hydrochloride **7** (4.86 g, 29 mmol) in dichloromethane (30 mL) under argon atmosphere was added dropwise triethylamine (4.2 mL, 30.5 mmol, 1.05 equiv) and the mixture was stirred at rt for 1 h.

To this mixture was added $MgSO_4$ (3 spatula tips) and pyvaldehyde (3.8 mL, 34.8 mmol, 1.2 equiv) and the reaction mixture was stirred at 50 °C for 15 h. The mixture was cooled at rt, filtered and the filtrate was concentrated in vacuum. The residue was dissolved in dichloromethane (30 mL), the resulting solution was washed with water (2 × 30 mL), dried on $MgSO_4$ and filtered. Evaporation of the solvents in vacuum afforded the imine **8a** (5.3 g, 26.6 mmol, 92%) as a colorless oil. $^1$H NMR (300 MHz, $CDCl_3$) $\delta$ 7.38 (s, 1H, NCH), 4.08 (quint, 2H, $J$ = 7.2 Hz, $CH_2$), 1.32 (s, 6H, $C(CH_3)_2$), 1.17 (t, 3H, $J$ = 7.2 Hz, $CH_2CH_3$), 0.97 (s, 9H, $C(CH_3)_3$); $^{13}$C NMR (75.5 MHz, $CDCl_3$) $\delta$ 174.8 (C=O), 169.4 (C=N), 64.5 ($C(CH_3)_2$), 60.6 ($CO_2CH_2$), 36.2 ($C(CH_3)_3$), 26.7 ($C(CH_3)_3$), 26.1 ($C(CH_3)_2$), 14.1 ($CO_2CH_2CH_3$). HRMS-ESI: calcd. for $C_{11}H_{22}NO_2^+$ $[M+H]^+$ 200.1645; found 200.1642.

A mixture of imine **8a** (200 mg, 1 mmol) and diethylphosphite (200 µL, 1.3 mmol, 1.3 equiv) was stirred inside a microwave reactor at 150 °C for 45 min. After cooling down to rt, the solution was diluted with dichloromethane (20 mL), washed with water (2 × 20 mL), dried over $MgSO_4$, filtered and evaporated in vacuum. The crude residue was purified by silica gel column chromatography eluting with pentane/acetone (5/1) to give **9a** as a colorless oil (250 mg; 74%). $^1$H NMR (300 MHz, $CDCl_3$) $\delta$ 4.12−3.93 (m, 6H, 3 × $CH_2CH_3$), 2.73 (d, 1H, $J$ = 17.4 Hz, CH), 1.28−1.18 (m, 15H, 2 × $POCH_2CH_3$, $CO_2CH_2CH_3$, 2 × $CH_3$), 0.97 (s, 9H, $C(CH_3)_3$); $^{13}$C NMR (75.5 MHz, $CDCl_3$) $\delta$ 176.2 (C=O), 61.3 (d, $J_{CP}$ = 7.2 Hz, $POCH_2$), 61.2 (d, $J_{CP}$ = 7.2 Hz, $POCH_2$), 60.2 ($CO_2CH_2$), 58.5 (d, $J_{CP}$ = 137.0 Hz, CH), 57.5 ($C(CH_3)_2$), 35.0 (d, $J_{CP}$ = 9.4 Hz, $C(CH_3)_3$), 27.7 (d, $J_{CP}$ = 6.1 Hz; $C(CH_3)_3$), 23.7 ($C(CH_3)_2$), 16.4 (d, $J_{CP}$ = 6.6 Hz, $POCH_2CH_3$), 14.0 ($CO_2CH_2CH_3$); $^{31}$P NMR (121.4 MHz, $CDCl_3$) $\delta$ 28.01. Anal. Calcd. for $C_{15}H_{32}NO_5P$: C, 53.40; H, 9.56; N, 4.15. Found: C, 53.00; H, 9.90; N, 4.15.

*Methyl 2-{[1-(diethoxyphosphoryl)-2-methylpropan-1-yl]-amino}-2-methylpropanoate (**9b**)*. To a solution of hydrochloride **7** (2 g, 12 mmol) in dichloromethane (12 mL) under argon atmosphere was added dropwise triethylamine (1.8 mL, 13.2 mmol, 1.05 equiv) and the mixture was stirred at rt for 1 h. To this mixture was added $MgSO_4$ (3 spatula tips) and isobutyraldehyde (2.4 mL, 14.4 mmol, 1.2 equiv) and the reaction mixture was stirred at 50 °C for 6 h. The mixture was cooled at rt, filtered and the

filtrate was concentrated in vacuum. The residue was dissolved in dichloromethane (30 mL), the resulting solution was washed with water (2 × 30 mL), dried on $MgSO_4$ and filtered. Evaporation of the solvents in vacuum afforded the imine **8b** (2.1 g, 11.4 mmol, 95%) as a colorless oil. $^1$H NMR (300 MHz, $CDCl_3$) $\delta$ 7.40 (d, $J$ = 6.0 Hz, 1H, NCH), 4.12 (quint, 2H, $J$ = 6.0 Hz, $CH_2$), 2.50−2.40 (m, 1H, C*H*$(CH_3)_2$), 1.37 (s, 6H, C$(CH_3)_2$), 1.21 (t, 3H, $J$ = 6.0 Hz, $CH_2CH_3$), 1.02 (m, 6H, CH$(CH_3)_2$); $^{13}$C NMR (75.5 MHz, $CDCl_3$) $\delta$ 176.6 (C=O), 167.9 (C=N), 64.5 (*C*$(CH_3)_2$), 60.7 ($CO_2CH_2$), 34.6 (CH), 26.0 (C$(CH_3)_2$), 19.2 (CH$(CH_3)_2$), 14.1 ($CO_2CH_2CH_3$). HRMS-ESI: calcd. for $C_{10}H_{20}NO_2^+$ $[M+H]^+$ 186.1489; found 186.1488.

A mixture of imine **8b** (400 mg, 2.16 mmol) and diethylphosphite (362 μL, 2.81 mmol) was stirred inside a microwave reactor at 150 °C for 30 min. After cooling down to rt, water (100 mL) was added and the mixture was treated with concentrated aqueous HCl until pH 2 and extracted with pentane (5 × 50 mL). The combined organic layers were dried over $MgSO_4$, filtered and evaporated in vacuum. The crude residue was purified by silica gel column chromatography eluting with pentane/acetone (5/1) to give **9b** as light yellow oil (650 mg; 68%). $^1$H NMR (300 MHz, $CDCl_3$) $\delta$ 4.15−4.08 (m, 6H, 3 × $CH_2CH_3$), 3.02 (dd, 1H, $J$ = 15.0 and 2.8 Hz, NHC*H*), 2.02−1.93 (m, 1H, C*H*$(CH_3)_2$), 1.32 (t, 3H, $J$ = 8.0 Hz, $POCH_2CH_3$), 1.30 (t, 3H, $J$ = 8.0 Hz, $POCH_2CH_3$), 1.29 (s, 6H, NHC$(CH_3)_2$), 1.27 (t, 3H, $J$ = 8.0 Hz, $CO_2CH_2CH_3$), 1.00 (d, 6H, $J$ = 8.0 Hz, CH$(CH_3)_2$); $^{13}$C NMR (75.5 MHz, $CDCl_3$) $\delta$ 176.8 (C=O), 62.2 (d, $J_{CP}$ = 7.5 Hz, $POCH_2$), 61.4 (d, $J_{CP}$ = 7.5 Hz, $POCH_2$), 60.6 ($CO_2CH_2$), 57.4 (d, $J_{CP}$ = 8.3 Hz, NH*C*$(CH_3)_2$), 55.2 (d, $J_{CP}$ = 148.6 Hz, CH), 30.1 (d, $J_{CP}$ = 6.8 Hz, *C*H$(CH_3)_2$), 26.5 (NHC*C*$H_3$), 25.5 (NHC*C*$H_3$), 19.2 (d, $J_{CP}$ = 10.6 Hz, CH*C*$H_3$), 18.7 (d, $J_{CP}$ = 10.6 Hz, CH*C*$H_3$), 16.5 (d, $J_{CP}$ = 6 Hz, $POCH_2CH_3$), 16.4 (d, $J_{CP}$ = 6 Hz, $POCH_2CH_3$), 14.0 ($CO_2CH_2CH_3$); $^{31}$P NMR (121.4 MHz, $CDCl_3$) $\delta$ 27.6. Anal. Calcd. for $C_{14}H_{30}NO_5P$: C, 52.00; H, 9.35; N, 4.33. Found: C, 52.36; H, 9.71; N, 4.19.

**Synthesis of Aminophosphonate Ester 16.** *(S)-Methylvaline ethyl ester hydrochloride (**14**).* This compound was prepared from (*S*)-methylvaline **13** (0.5 g, 3.82 mmol) and acetyl chloride (870 μL, 12.2 mmol, 3.2 equiv) in ethanol (5 mL) according to the procedure used for preparing **7**, with a reaction

time of 72 h. Compound **14** was obtained as a white powder (745 mg, 3.81 mmol, quantitative yield); mp 121.0−121.5 ° C; $[\alpha]^{25}_{D} = -13.5°$ (0.01, $H_2O$). $^1$H NMR (300 MHz, $D_2O$) $\delta$ 4.21 (q, $J$ = 7.0 Hz, 2H, $CH_2$), 2.14 (m, 1H, C*H*$(CH_3)_2$), 1.45 (s, 3H, $CH_3$), 1.21 (t, 3H, $J$ = 7.0 Hz, $CH_2CH_3$), 0.91 (br s, 6H, $CH(CH_3)_2$); $^{13}$C NMR (75.5 MHz, $CDCl_3$) $\delta$ 172.0 (C=O), 66.0 ($C_\alpha$), 63.7 ($CO_2CH_2$), 34.0 ($CH(CH_3)_2$), 18.9 ($C_\alpha(CH_3)$), 16.2 ($C(CH_3)_2$), 15.4 ($C(CH_3)_2$), 13.1 ($CO_2CH_2CH_3$).

*Methyl 2-{[1-(diethoxyphosphoryl)-2,2-dimethylpropan-1-yl]-amino}-2,3-dimethylbutanoate (**16**)*. To a solution of hydrochloride **14** (745 mg, 3.82 mmol) in dichloromethane (5 mL) under argon atmosphere was added dropwise triethylamine (558 µL, 4.01 mmol, 1.05 equiv) and the mixture was stirred at rt for 1 h. To this mixture was added $MgSO_4$ (3 spatula tips) and pyvaldehyde (500 µL, 4.6 mmol, 1.2 equiv) and the reaction mixture was stirred at rt for 72 h. The mixture was filtered, the filtrate concentrated in vacuum, then diluted in dichloromethane (10 mL). The solution was washed with water (2 × 10 mL), dried on $MgSO_4$ and filtered. Evaporation of the solvents in vacuum afforded the imine **15** (563 mg, 2.48 mmol, 65%) as a colorless oil. $^1$H NMR (300 MHz, $CDCl_3$) $\delta$ 7.37 (s, 1H, NCH), 4.08 (quint, 2H, $J$ = 7.3 Hz, $CH_2$), 2.16 (hept, 1H, $J$ = 6.8 Hz, C*H*$(CH_3)_2$), 1.17 (t, 3H, $J$ = 7.3 Hz, $CO_2CH_2CH_3$), 1.14 (s, 3H, $C(CH_3)$), 0.97 (s, 9H, $C(CH_3)_3$), 0.85 (d, 3H, $J$ = 6.8 Hz, $CH(CH_3)_2$), 0.77 (d, 3H, $J$ = 6.8 Hz, $CH(CH_3)_2$); $^{13}$C NMR (75.5 MHz, $CDCl_3$) $\delta$ 174.5 (C=O), 169.5 (C=N), 70.4 ($C_\alpha$), 60.2 ($CO_2CH_2$), 36.5($CH(CH_3)_2$), 35.5 ($C(CH_3)_3$), 26.6 ($C(CH_3)_3$), 18.6 ($C_\alpha(CH_3)$), 17.3 and 16.9 ($CH(CH_3)_2$), 14.1 ($CO_2CH_2CH_3$); HRMS-ESI: calcd. for $C_{13}H_{26}NO_2^+$ $[M+H]^+$ 228.1958; found: 228.1953.

A mixture of imine **15** (0.5 g, 2.20 mmol) and diethylphosphite (400 µL, 2.86 mmol, 1.3 equiv) was stirred for 15 days at 55 °C in a sealed vessel. After cooling down to rt, the mixture was diluted with dichloromethane (20 mL), washed with water (2 × 20 mL), dried over $MgSO_4$, filtered and evaporated in vacuum. The crude residue was purified by silica gel column chromatography eluting with pentane/acetone (5/1) to give compound **16** as a colorless oil (300 mg; 37%) containing a 1:1 ratio of diastereomers (determined by HPLC). Anal. Calcd. for $C_{17}H_{36}NO_5P$: C, 55.87; H, 9.93; N, 3.83. Found: C, 55.97; H, 9.99; N, 3.75.

**Separation of the Two Diastereomers of 16.** The two diastereomers were separated by chiral column chromatography under the following conditions: column, Chiralpak IC, 250 mm × 10 mm; mobile phase, hexane/isopropanol/chloroform (8/1/1); flow rate, 5 mL/min; sample concentration, 300 mg/10 mL in hexane/isopropanol/chloroform (4/3/3); injected volume per run, 230 μL injected 45 times every 4.5 min; UV detection at 230 nm.

First eluted diastereomer ($t_R$ = 4.87 min) (2*S*,1'*R*)-**16**: $[\alpha]^{25}_D$ = +28.8° (0.034, $CHCl_3$). $^1H$ (300 MHz, $CDCl_3$) $\delta$ 4.24−4.02 (m, 6H, 3 × C$H_2$CH$_3$), 2.73 (d, 1H, $J$ = 16.3 Hz, CH), 1.82 (hept, 1H, $J$ = 6.8 Hz, C$H$(CH$_3$)$_2$), 1.36−1.27 (m, 9H, 2 × POCH$_2$C$H_3$, CO$_2$CH$_2$C$H_3$), 1.11 (s, 3H, CCH$_3$), 1.09 (s, 9H, C(CH$_3$)$_3$), 0.98 (d, 3H, $J$ = 6.8 Hz, CH(C$H_3$)$_2$), 0.83 (d, 3H, $J$ = 6.8 Hz, CH(C$H_3$)$_2$); $^{13}C$ NMR (75.5 MHz, $CDCl_3$) $\delta$ 176.0 (C=O), 63.5 (CO$_2$*C*H$_2$), 61.5 (d, $J_{CP}$ = 6.6 Hz, POCH$_2$), 60.6 (d, $J_{CP}$ = 7.7 Hz, POCH$_2$), 60.0 (C$H$(CH$_3$)$_2$), 57.9 (d, $J_{CP}$ = 129.9 Hz, CH), 38.8 (d, $J_{CP}$ = 2.8 Hz, *C*(CH$_3$)$_3$), 35.7 (d, $J_{CP}$ = 9.9 Hz; C(*C*H$_3$)$_3$), 28.2 (CH(*C*H$_3$)$_2$), 28.1 (CH(*C*H$_3$)$_2$), 23.5 (C(*C*H$_3$)*i*Pr), 20.2 (*C*(CH$_3$)*i*Pr), 17.6 (d, $J_{CP}$ = 7.2 Hz, POCH$_2$*C*H$_3$), 16.9 (d, $J_{CP}$ = 8.2 Hz, POCH$_2$*C*H$_3$), 14.0 (CO$_2$CH$_2$*C*H$_3$); $^{31}P$ NMR (121.4 MHz, $CDCl_3$) $\delta$ 28.08.

Second eluted diastereomer ($t_R$ = 6.05 min) (2*S*,1'*S*)-**16**: $[\alpha]^{25}_D$ = −14.5° (0.014, $CHCl_3$); $^1H$ (300 MHz, $CDCl_3$) $\delta$ 4.08−3.98 (m, 6H, 3 × C$H_2$CH$_3$), 2.95 (d, 1H, $J$ = 19.1 Hz, CH), 1.91 (hept, 1H, $J$ = 6.8 Hz, C$H$(CH$_3$)$_2$), 1.26 (t, 3H, $J$ = 6.9 Hz, POCH$_2$C$H_3$), 1.25 (t, 3H, $J$ = 6.9 Hz, POCH$_2$C$H_3$), 1.21 (t, 3H, $J$ = 7.2 Hz, CO$_2$CH$_2$C$H_3$), 1.11 (s, 3H, CCH$_3$), 0.95 (s, 9H, C(CH$_3$)$_3$), 0.91 (d, 3H, $J$ = 6.8 Hz, CH(C$H_3$)$_2$), 0.76 (d, 3H, $J$ = 6.8 Hz, CH(C$H_3$)$_2$); $^{13}C$ NMR (75.5 MHz, $CDCl_3$) $\delta$ 176.3 (C=O), 61.8 (d, $J_{CP}$ = 6.2 Hz, POCH$_2$), 61.2 (d, $J_{CP}$ = 7.7 Hz, POCH$_2$), 61.0 (CO$_2$*C*H$_2$), 60.5 (C$H$(CH$_3$)$_2$), 59.4 (d, $J_{CP}$ = 132.1 Hz, CH), 37.4 (br s, *C*(CH$_3$)$_3$), 35.4 (d, $J_{CP}$ = 10.5 Hz; C(*C*H$_3$)$_3$), 28.9 (CH(*C*H$_3$)$_2$), 28.8 (CH(*C*H$_3$)$_2$), 23.4 (C(*C*H$_3$)*i*Pr), 20.2 (*C*(CH$_3$)*i*Pr), 16.8 (d, $J_{CP}$ = 6.2 Hz, POCH$_2$*C*H$_3$), 16.5 (d, $J_{CP}$ = 5.5 Hz, POCH$_2$*C*H$_3$), 14.1 (CO$_2$CH$_2$*C*H$_3$); $^{31}P$ NMR (121.4 MHz, $CDCl_3$) $\delta$ 27.08.

**General Procedure for the Synthesis of Nitroxides β-Esters 10a, 12 and 17.** The corresponding aminoester (1 equiv) was dissolved in a volume of chloroform as to give a final concentration of 250

mM. This solution was cooled at 0 °C and a solution of *m*-CPBA (2 equiv) in chloroform (same volume) was added dropwise in 2 h. The mixture was stirred for 2 h at 0 °C then the organic layer was washed with saturated aqueous $Na_2CO_3$ (3 × 4 mL) and by brine (4 mL). The organic layer was dried over $MgSO_4$, filtered and evaporated in vacuum to give the crude nitroxides β-esters.

*N-(ethyl-2-methylpropanoate)-(1-diethoxyphosphoryl-2,2-dimethylpropyl) nitroxide (**10a**)*. Title compound was prepared from solutions of **9a** (250 mg, 0.73 mmol) and *m*-CPBA (360 mg, 1.5 mmol), both in chloroform (3 mL). Purification of the crude residue by silica gel column chromatography eluting with dichloromethane/acetone (5/1) afforded **10a** as an orange oil (197 mg, 80%). Anal. Calcd. for $C_{15}H_{32}NO_6P$: C, 51.13; H, 8.87; N, 3.97. Found: C, 51.19; H, 9.34; N, 3.93.

*N-(ethyl-2-methylpropanoate)-(1-diethoxyphosphoryl-2-methylpropyl) nitroxide (**12**)*. Title compound was prepared from solutions of **9b** (30 mg, 0.09 mmol) and *m*-CPBA (46 mg, 0.19 mmol), both in chloroform (1 mL). Compound **12** was obtained as pale orange oil (32 mg, quantitative yield). HRMS-ESI: calcd. for $C_{14}H_{30}NO_6P\bullet$ $[M+H]^+$ 339.1805; found 339.1802. Anal. Calcd. for $C_{14}H_{29}NO_6P$: C, 49.70; H, 8.64; N, 4.14. Found: C, 51.10; H, 8.97; N, 3.93.

*N-(ethyl-2,3-dimethylbutanoate)-(1-diethoxyphosphoryl-2,2-dimethylpropyl) nitroxide* ((2*S,*1'*R*)-***17***). Title compound was prepared from solutions of (2*S,*1'*R*)-**16** (110 mg, 0.30 mmol) and *m*-CPBA (149 mg, 0.60 mmol), both in chloroform (1.5 mL). Compound (2*S,*1'*R*)-**17** was obtained as a pale orange oil (67 mg, 60%). HRMS-ESI: calcd. for $C_{17}H_{36}NO_6P\bullet$ $[M+H]^+$ 381.2275; found 381.2274. Anal. Calcd. for $C_{17}H_{35}NO_6P$: C, 53.67; H, 9.27; N, 3.68. Found: C, 53.97; H, 9.04; N, 3.93.

*N-(ethyl-2,3-dimethylbutanoate)-(1-diethoxyphosphoryl-2,2-dimethylpropyl) nitroxide* ((2*S,*1'*S*)-***17***). Title compound was prepared from solutions of (2*S,*1'*S*)-**16** (80 mg, 0.22 mmol) and *m*-CPBA (108 mg, 0.44 mmol), both in chloroform (1 mL). Compound (2*S,*1'*S*)-**17** was obtained as a pale orange oil (54 mg, 65%). HRMS-ESI: calcd. for $C_{17}H_{36}NO_6P\bullet$ $[M+H]^+$ 381.2275; found 381.2274. Anal. Calcd. for $C_{17}H_{35}NO_6P$: C, 53.67; H, 9.27; N, 3.68. Found: C, 53.75; H, 9.23; N, 3.72.

***N-2-(2-methylpropanoate)-(1-diethoxyphosphoryl-2,2-dimethylpropyl) nitroxide sodium salt (10b*).** Nitroxide **10a** (197 mg, 0.6 mmol) was dissolved in a 5 M aqueous NaOH (1.2 mL, 10 equiv) and stirred vigorously for 15 h at rt. The mixture was extracted with dichloromethane (4 × 5 mL), the organic layers were gathered, dried over $MgSO_4$, filtrered and concentrated in vacuum. The resulting crude residue was precipitated with pentane to give a precipitate which was filtered, affording **10b** as yellow crystals (81 mg, 42%); mp 111.6−112.0 °C. Anal. Calcd. for $C_{13}H_{26}NO_6PNa$: C, 45.09; H, 7.57; N, 4.0. Found: C, 45.45; H, 7.58; N, 4.33.

**In Situ Formation of Carboxylic Nitroxide 11b.** *N-2-(2-methylpropan)-(1-diethoxyphosphoryl-2-methylpropyl)-oic acid (**11a**)*. Ester **9b** (0.1 g, 310 μmol) was saponified according to the procedure used to prepare **10b**, affording carboxylic acid **11a** as a yellow oil (91 mg, quantitative yield). $^1$H (300 MHz, $CDCl_3$) $\delta$ 6.43 (br s, 2H, $CO_2H$ and NH), 4.18−4.08 (m, 4H, 2 × C$H_2$CH$_3$), 3.04 (dd, 1H, $J$ = 18.3 and 2.9 Hz, NHC*H*), 2.08 (m, 1H, C*H*(CH$_3$)$_2$), 1.37−1.29 (m, 12H, 2 × POCH$_2$C$H_3$ and NHC(C$H_3$)$_2$), 1.03 (d, 3H, $J$ = 6.0 Hz, CH(C$H_3$)$_2$), 1.01 (d, 3H, $J$ = 6.0 Hz, CH(C$H_3$)$_2$); $^{13}$C NMR (75.5 MHz, $CDCl_3$) $\delta$ 178.5 (C=O), 65.6 ($CO_2CH_2$), 62.2 (d, $J_{CP}$ = 8.3 Hz, $POCH_2$), 62.1 (d, $J_{CP}$ = 8.3 Hz, $POCH_2$), 58.4 (d, $J_{CP}$ = 8.8 Hz, NH*C*(CH$_3$)$_2$), 55.1 (d, $J_{CP}$ = 151.3 Hz, CH), 29.8 (d, $J_{CP}$ = 5.0 Hz, *C*H(CH$_3$)$_2$), 26.2 (NHC*C*H$_3$), 24.6 (NHC*C*H$_3$), 19.2 (d, $J_{CP}$ = 11.0 Hz, CH*C*H$_3$), 18.7 (d, $J_{CP}$ = 10.6 Hz, CH*C*H$_3$), 16.2 (d, $J_{CP}$ = 1.6 Hz, POCH$_2$*C*H$_3$), 16.1 (d, $J_{CP}$ = 1.6 Hz, POCH$_2$*C*H$_3$); $^{31}$P NMR (121.4 MHz, $CDCl_3$) $\delta$ 27.1; HRMS-ESI: calcd. for $C_{12}H_{27}NO_5P^+$ $[M+H]^+$ 296.1621; found 296.1623. Anal. Calcd. for $C_{12}H_{26}NO_5P$: C, 48.81; H, 8.87; N, 4.74. Found: C, 49.13; H, 8.98; N, 4.45.

*N-2-(2-methylpropan)-(1-diethoxyphosphoryl-2-methylpropyl)-oic acid oxide (**11b**)*. Title compound was formed in situ from **11a** according to the procedure used for **5a**,**c** and the resulting nitroxide working solution in 20 mM phosphate buffer can be used in EPR titration experiments within 3−4 h following addition of oxidant. Using a calibration curve established with 0.01−0.1 mM TMPPO, the initial concentration of the working solutions of nitroxides **5a**,**c** and **11b** prepared in situ was found ranging 0.05−0.1 mM.

**X-ray Diffraction Analysis.** X-ray diffraction data were collected at 293 K on a Bruker-Nonius Kappa CCD diffractometer using graphite-monochromated Mo Kα radiation (λ = 0.71073 Å).

Cystal data for **10b**: $C_{13}H_{26}NNaO_6P$ $M$ = 347.31 monoclinic space group C2/c, Hall group –C 2yc, a = 22.2170(5), b = 16.2403(5), c = 10.8482(3) Å, β = 91.788(2)°.

Crystallographic data for the structure of **10b** have been deposited at the Cambridge Crystallographic Data Center with the deposition number number 793807. This material can be obtained free of charge at www.ccdc.cam.uk/conts/retrieving.html or from the CCDC at deposit@ccdc.cam.ac.uk.

**$^{31}$P NMR pH-Calibration of α-Aminophosphonate Esters 3a−c, 9a,b and diastereomers of 16.** Calibration experiments were carried out in the following media: phosphate buffer (1 mM $KH_2PO_4$), KH (containing: 118.5 mM NaCl, 4.8 mM KCl, 1.2 mM $MgSO_4$, 25 mM $NaHCO_3$ and 1.2 mM $KH_2PO_4$) having a ionic strength of 0.154, or homogenates $CytM_l$ or $CytM_h$.[10a,31] Test compounds (5 mM) were dissolved in the selected medium and the pH was adjusted to 15−20 different values in the range 1.0−12.0 with 1 N solutions of HCl or NaOH. The pH was measured using a SevenCompact digital pH-meter equipped with an Inlab Micro Pro micro-electrode (Mettler Toledo, Switzerland).

The $^{31}$P NMR spectra of titration solutions were acquired (32 accumulated scans) at 22 °C on either Bruker AMX 400 (at 161.9 MHz) or Avance I 500 MHz (at 202.46 MHz) instruments equipped with 10- or 5-mm probes, respectively. The chemical shifts (referenced to external 85% $H_3PO_4$ at 0 ppm) were plotted against pH to fit the Henderson-Hasselbalch equation for NMR using a nonlinear regression:

$$\mathrm{pH} = \mathrm{p}K_a + \log\frac{d - d_a}{d_b - d} \qquad (2)$$

where $\delta$ is the experimental $^{31}$P chemical shift and $\delta_a$ and $\delta_b$ correspond to the limiting chemical shift values of the protonated and unprotonated form, respectively. The $T_1$ values were determined at pH ≈ p$K_a$ using a standard inversion / recovery (180°−τ−90°)−TR pulse-sequence with a 180° composite pulse, with the repetition time TR being 6−7 times the $T_1$ value. The number of scans was 8 and 16

evolution decays (τ) were used. For both diastereomers of **16** $T_1$ was measured at pH 4.00. Data are means of 3−10 repeated titrations.

**Molecular Dynamics Simulations.** All calculations were performed using GROMACS 5.0.5 package.[34] The best conformer of the protonated and unprotonated forms of each titrating nitroxide was fully optimized at the PBE0/6-31+G(d,p) level using the ab initio program Gaussian 09 revision D.01 package.[35] Each nitroxide was solvated in a quasi-cubic box containing about 800 water molecules. In the case of unprotonated species the net charge of the system was neutralized with one sodium ion. The force fields employed in the simulations were TIP3P[36] (description of the water molecules) and AMBER (ff99SB)[37] including additional parameters for nitroxide moieties.[38] The atomic charges were computed at the HF/6-31G(d) level of theory with the RESP scheme.[39] To optimize the simulation box size a NPT calculation was performed at 300 K and 1 bar during 200 ps with a time step of 0.5 fs. After this first stage, a NVT trajectory was performed at 300 K during 100 ns with a time step of 0.5 fs. The last 99.5 ns of the trajectory were kept in the simulation and the data analysis calculations were performed on 99500 structures with system coordinates saved every 1 ps.

**In Vitro EPR Experiments.** *General.* All EPR measurements were performed at 22 °C unless otherwise noted, using an X-band (9.79 GHz) Bruker ESP 300 spectrometer (Karlsruhe, Germany) with a $TM_{110}$ microwave cavity, using a modulation frequency of 100 KHz and a microwave power of 10 mW. The magnetic field strength and microwave frequency were measured with a Bruker ER 035M proton probe gaussmeter and a Hewlett-Packard 5350B frequency meter, respectively. The temperature inside the resonant cavity was controlled by a Bruker ER 4111VT variable temperature unit. Coupling constants and *g*-factors were determined by computer simulation of spectra having 4k resolution using the program of Rockenbauer and Korecz.[40] In order to resolve long-range EPR couplings, samples were deoxygenated by argon bubbling before their transfer into 50 μL glass capillary tubes sealed at both ends with Critoseal. To optimize signal resolution of each tested nitroxide, other instrument settings were adjusted within the following ranges: modulation amplitude, 0.02−0.48 G; time constant,

5.12−81.92 ms; receiver gain, $2.5 \times 10^4$−$2 \times 10^5$; scan rate, 0.25−1.51 G/s; sweep width, 83−110 G (see also Figure legends).

*EPR pH-Calibration.* Working solutions of the nitroxides **5a**,**c** and **11b** prepared in situ as described above or aqueous stock solutions of isolated nitroxides prepared by weighing and diluted in appropriate solvent to yield a final concentration of 0.05 mM (**10b**), 1 mM (**10a**, **12**) or 3 mM (diastereomers of **17**) were used in calibration experiments. The pH was serially adjusted to 10−15 different values in the range 0.5−12.0 with 1 N HCl or NaOH, and the EPR scan was initiated at room temperature 90 s following stabilization of the pH.

The plot of hfs as a function of pH as determined from spectral simulations of experimental EPR spectra yielded the p$K_a$ value and the EPR sensitivity $\Delta a_X$ for **5a**,**c**, **10b** and **11b** using the Henderson-Hasselbalch equation for EPR

$$\mathrm{pH} = \mathrm{p}K_a + \log \frac{a_X - (a_X)_a}{(a_X)_b - a_X} \qquad (3)$$

where $a_X$ is the experimental coupling constant of the nucleus X, and $(a_X)_a$ and $(a_X)_b$ are the corresponding limiting coupling constants in the protonated and unprotonated form of the nitroxide, respectively. Data are means of 3 repeated titrations.

*Bioreduction of **10b**, TMPPO and 3-CP*. Twenty microliters of an aqueous stock solution of tested compound were diluted with an aliquot (80 μL) of $CytM_l$ in either KH buffer, pH 7.0 or a phosphate-citrate buffer (0.25 M; pH 3.5) to reach a final nitroxide concentration of 0.1 mM (see preparation below). The mixture was vortexed for 10 s, transferred into a glass capillary and the decay of EPR double integrated simulations was monitored over time at 37 °C. Spectral acquisition was started 1 min after mixing using the settings: modulation amplitude, 0.31−0.48 G; time constant, 20.48 ms; receiver gain, 1−4 × $10^5$; scan rate, 2.4−4.8 G/s; sweep width, 50 G (for 3-CP) or 100 G (for **10b** and TMPPO). For each nitroxide data ± SD were computed from at least 5 independent determinations in each medium.

**Biology.** *Reagents*. Doubly distilled deionized water was used throughout. Dulbecco's modified Eagle's medium (DMEM), phosphate buffered saline (PBS), fetal calf serum (FCS), antibiotics and antimycotic agents were from Gibco Life Technologies (Thermo Fisher Scientific, Saint Aubin, France). Stock solutions were freshly diluted in the appropriate culture medium prior to use and filtered through a 0.2-μm Millipore filter.

*Cell Culture and Exposure.* Cell culture was performed according to the conditions described earlier.[30] Briefly, human alveolar epithelial A549 cells (CCL-185; ATCC, LGC Standards, Molsheim, France) were grown in DMEM containing 10% FCS, 100 U/mL penicillin, 100 μg/mL streptomycin and 2 mM GlutaMax (Gibco) at 37 °C in a 5% $CO_2$ humidified atmosphere. NHLF (Lonza, Amboise, France) were seeded in culture dishes and incubated in fibroblast basal medium (FBM; Lonza) supplemented by growth factors (FGM; Clonetics FGM-2 Bullet Kit; Lonza). The exponential growth phase of the cells was performed at 37 °C in 5% $CO_2$ humidified atmosphere and the culture medium was renewed every two days. Confluent cells (in 25 $cm^2$ flasks) were trypsinized, seeded onto 96-well plates (at a density of $2.5 \times 10^4$ cells/well) and incubated up to confluence in appropriate medium. The medium was renewed and cells were exposed to varying concentrations of test compounds for 48 h in wells containing the appropriate medium.

*Evaluation of Cytotoxicity*. Following exposure 10 μL of medium was removed from each well to determine LDH activity released into the incubation medium according to the instructions of the Biolabo LDH kit (Maizy, France). The total cellular LDH content was obtained by treating control wells with Triton X-100 (1% final) to induce 100% loss of viability and total LDH release. After removal of the remaining incubation medium cells were washed two times with PBS 1X (+/+) and cytotoxicity was determined using the fluorometric microculture cytotoxicity assay (FMCA)[30] and the 3-(4,5-dimethyl-2-thiazolyl)-2,5-diphenyl-2*H*-tetrazolium bromide (MTT) assay.

*FMCA Assay*. Once washed, cells in each well were incubated at 37 °C for 30 min with 220 μL PBS 1X (+/+) containing fluorescein diacetate (4.8 μM; Sigma-Aldrich). After addition of Triton X-100 (3%

final) incubation was prolonged for 5 min under stirring and the mixture was transferred onto 96-well black plates for fluorescence determination at 535 nm, following excitation at 485 nm. For each test compound, dose-response curves were established from at least 4 different concentrations made in triplicate, and $IC_{50}$ values were obtained as the concentration inhibiting 50% of fluorescence.

*MTT Assay*. An aliquot of 100 µL PBS 1X (+/+) containing 0.5 mg/mL MTT (Acros) was reloaded onto the wells and incubation was extended for 2 h at 37 °C. The medium was replaced by 100 µL/well DMSO and incubation was prolonged for 15 min at room temperature under stirring. The conversion of MTT to a purple formazan precipitate was monitored at 570 nm. The inhibition of cell viability was calculated as $IC_{50}$ values using regression calculations from at least 4 different concentrations made in triplicate.

*Animal Procedures and Ethics*. Seventeen Sprague-Dawley male rats weighing ~450 g (CERJ, Le Genest St Isle, France) were used in the study. Rats were maintained in the local animal house under conventional conditions including an enrichment of the structural and social environment while promoting physical and cognitive activity, in a room with controlled temperature (22 ± 3 °C) and a reverse 12 h light/dark cycle with food (standard Teklad 2016 diet, Harlan Laboratories, Gannat, France) and water available ad libitum. All research involving animals were performed in strict compliance with the guidelines of the Directive 2010/63/EU of the European Parliament. The CNRS and Aix Marseille Université have currently valid license for animal housing and experimentation (agreement C13-055-06) delivered by the French Government and the study was under the supervision of a DVM at CNRS (agreement N°13-122). The protocol was approved by the National Research Committee for the project.

*Preparation of Rat Organ Homogenates.* Heart, liver or stomach extracts were prepared from freshly excised organs as previously described.[10a] Briefly, 8 g of tissue were minced in 12 mL of 125 mM KCl at 2 °C, homogenized in a blender for 10 min and centrifuged at 10,000 × g for 20 min at 2−3 °C. The clear supernatant solution taken as a cytosolic–like medium was used for $^{31}P$ NMR titrations. For EPR

bioreduction assays rat liver homogenates were prepared by mixing in a blender 2 g of freshly excised tissue with 6 mL of either KH buffer (pH 7.0) or phosphate-citrate buffer (0.25 M, pH 3.5).

*pH Measurement in the Rat Stomach Fluid.* Rats fasted for 10 h were anesthetized with 3% sevoflurane using previously described procedures[41] and instrumented with a thin teflon cannula inserted into the stomach. This allowed administration of 3.5 mL aliquots of **3a** (5 mM) or **10b** (3 mM) dissolved in 5 mM phosphate buffer (pH 7.01; to keep physiological conditions), 100 mM bicarbonate buffer (pH 8.27), or a 1:1 dilution of Maalox in water (pH 8.67). Maalox, a solid formulation of 34.9 mg/mL of $Al(OH)_3$ and 39.9 mg/mL of $Mg(OH)_2$, was form Theraplix (France).

Five min after drug administration the gastric medium (0.5 mL) was drawn and the pH was measured using a pH microelectrode. After 30 min equilibration samples of the stomach fluid containing **3a** (~2 mL) or **10b** (~0.5 mL) were drawn, scanned by $^{31}P$ NMR or EPR, respectively (see below), and the pH calculated from the corresponding titration curves. In parallel, the pH of each gastric fluid was measured with a pH electrode. $^{31}P$ NMR spectra were acquired from 2 mL samples of stomach fluid on a Bruker AVL 400 (at 162 MHz) instrument equipped with a 10-mm probe and using sequences of at least 64 accumulated scans. EPR analysis was carried out 3 min after the end of sampling using the following settings: modulation amplitude, 0.088 G; time constant, 20.48 ms; receiver gain, $8 \times 10^4$; scan rate, 1.13 G/s; sweep width, 95 G.

During anesthesia heart function was monitored by the tail-cuff method using a Letica Scientific LE 5000/5500 instrument (Barcelona, Spain) and a programmed electrosphygmomanometer (LE 5160-R; Panlab, Barcelona, Spain). At the end of experiments animals were kept alive and no mortality associated with anesthesia and compound toxicity was observed in the long term. Data represent means ± SEM with $n = 3-7$ (electrode) or $n = 7$ (spectroscopic measurements) / experimental condition.

**Data Calculations and Statistics.** Titration curves were obtained using Prism 5.0 software (GraphPad, San Diego, CA). Data are expressed as mean ± SD or SEM for the indicated number of independent experiments. Differences were analyzed using a one-way analysis of variance (ANOVA)

followed by a posteriori Newman–Keuls test. Intergroup differences were considered to be significant at $P < 0.05$.

**Acknowledgments**

The authors thank S. Gonzales-Calera and S. Martel for expert assistance, and N. Vanthuyne for chiral analytical HPLC studies. This work was supported by the computing facilities of the CRCMM (Centre Régional de Compétences en Modélisation Moléculaire de Marseille) and the research was financially supported by the Agence Nationale pour la Recherche (ANR-09-BLAN-005-03) and grants from the project FEDER-AdiabaOx (2008, n° 13851).

This article is dedicated to the memory of our colleague François Le Moigne.

FIGURE CAPTIONS

**Figure 1.** (A) $^{31}$P NMR pH probes and their p$K_a$s in Krebs-Henseleit buffer.[9a,9b,10b] (B) EPR pH probes with their reported p$K_a$s and sensitivities in Tris-HCl buffer.[12,13a] (C) General structure of target carboxylic EPR pH probes showing preferred resonance forms of ionization states. Left panel: structurally related pH insensitive DEPN and crystallized derivatives.

**Figure 2.** (A) ORTEP view of **10b** showing the nitroxide function and the atoms and dihedral angles implicated in the Heller-McConnell relation. Thermal ellipsoids represent 50% equiprobability envelopes. (B) Newman projection along the N−C$_\alpha$, axis.

**Figure 3.** (A) EPR spectrum of **10b** (1 mM) in degassed phosphate buffer (20 mM; pH 7.21) showing long-range hydrogen couplings (expanded region with simulation) and two $^{13}$C satellites (arrows). Settings: modulation amplitude, 0.03 G; time constant, 20.48 ms; gain, $3.2 \times 10^4$; scan rate, 0.57 G/s,

accumulated scans, 10. (B) Limiting protonated and unprotonated EPR spectra of **10b** (0.36 mM) and **5c** (~0.1 mM) in 20 mM phosphate buffer. Settings (**10b**, **5c**): modulation amplitude, (0.06, 0.48) G; time constant, (40.96, 5.12) ms; gain, ($1 \times 10^5$, $4 \times 10^4$); scan rate, (1.13, 1.31) G/s. Signals of **5c** were recorded in the reaction mixture 4 min (pH 6.25) and 40 min (pH 1.64) following oxidation of amine **4c** by *m*-CPBA. The vertical lines allow a visual comparison of differences in $a_P$ values.

**Figure 4.** EPR pH titration curves for **10b** in phosphate buffer at 22 °C.

**Figure 5.** Reduction of nitroxides (0.1 mM) by cytosolic rat liver homogenate at 37 °C in phosphate-citrate buffer, pH 3.5 or Krebs-Henseleit medium, pH 7.0. $I_0$ is the initial intensity of the EPR signal recorded 1 min after mixing.

**Figure 6.** Low-field lines of EPR spectra recorded from the gastric fluid of a resting rat 30 min after receiving a solution of **10b** (3 mM) in (a) 5 mM phosphate buffer (pH 7.0), (b) Maalox:water (1:1, v/v; pH 8.7), or (c) 0.1 M sodium bicarbonate (pH 8.4) via a cannula inserted into the stomach. (B) Mean value ± SEM ($n$ = 3−7/group) of gastric pH measured 30 min after drug administration using a pH electrode, or by EPR (from $a_P$ coupling) or $^{31}$P NMR using **10b** (3 mM) or **3a** (5 mM) as pH probes, respectively. Starting pH values at 5 min correspond to animals given **10b**.

**Abbreviations used**

$\delta_a$, limiting chemical shift of the protonated form; $\delta_b$, limiting chemical shift of the unprotonated form; $\Delta\delta_{ab} = \delta_a - \delta_b$; 3-CP, 3-carboxy-2,2,5,5-tetramethylpyrrolidine 1-oxyl; $CytM_h$, heart cytosolic homogenate; $CytM_l$, liver cytosolic homogenate; $CytM_s$, rat stomach cytosolic medium; *m*-CPBA, *m*-chloroperoxybenzoic acid; DEPMPH, diethyl(2-methylpyrrolidin-2-yl) phosphonate; DEPN, *N-tert*-

butyl-*N*-[1-diethylphosphono(2,2-dimethylpropyl)] nitroxide; DMEM, Dulbecco's modified Eagle's medium; DPP, diethyl(2-propylaminoprop-2-yl)phosphonate; FCS, fetal calf serum; FGM, fibroblast basal medium; KH, Krebs-Henseleit; LDH, lactate dehydrogenase; MD, molecular dynamics; $pH_i$, intracellular pH; $P_i$, inorganic phosphate; PBS, phosphate-buffered saline; TEMPO, 2,2,6,6-tetramethylpiperidine 1-oxyl; TMPPO, 2-diethoxyphosphoryl-2,5,5-trimethylpyrrolidine 1-oxyl.

**Associated Content**

**Supporting Information.** ROESY spectra of diastereomers of compound **16**; $^{31}$P NMR acid-base titration curves of compounds **3a** and **9a**,**b**; Additional EPR pH titration curves of compounds **5a**,**c**; Additional molecular dynamics data.

**References**

(1) (a) Boron, W. F. Regulation of intracellular pH. *Adv. Physiol. Educ*. **2004**, *28*, 160−179. (b) Casey, J. R.; Grinstein, S.; Orlowski, J. Sensors and regulators of intracellular pH. *Nat. Rev. Mol. Cell. Biol.* **2010**, *11*, 50−161.

(2) (a) Anderson, G. W.; Orci, L. A view of acidic intracellular compartments. *J. Cell Biol*. **1988**, *106*, 539−543. (b) Llopis, J.; McCaffery, J. M.; Miyawaki, A.; Farquhar, M. G.; Tsien, R. Y. Measurement of cytosolic, mitochondrial, and Golgi pH in single living cells with green fluorescent proteins. *Proc. Natl. Acad. Sci. U.S.A*. **1998**, *95*, 6803−6808.

(3) Mulkey, D. K.; Henderson, R. A. 3rd; Ritucci, N. A.; Putnam, R. W.; Dean, J. B. Oxidative stress decreases pHi and Na(+)/H(+) exchange and increases excitability of solitary complex neurons from rat brain slices. *Am. J. Physiol. Cell. Physiol*. **2004**, *286*, C940−C951.

(4) Lagadic-Gossmann, D.; Huc, L.; Lecureur, V. Alterations of intracellular pH homeostasis in apoptosis: origins and roles. *Cell Death Differ.* **2004**, *11*, 953−961.

(5) Webb, B. A.; Chimenti, M.; Jacobson, M.P.; Barber, D. L. Dysregulated pH: A perfect storm for cancer progression. *Nat. Rev. Cancer* **2011**, *11*, 671−677.

(6) Khramtsov, V. V. Biological imaging and spectroscopy of pH. *Curr. Org. Chem*. **2005**, *9*, 909−923.

(7) (a) Han, J.; Burgess, K. Fluorescent indicators for intracellular pH. *Chem. Rev.* **2010**, *110*, 2709−2728. (b) Wang, R.; Yu, C.; Yu, F.; Chen, L. Molecular fluorescent probes for monitoring pH changes in living cells. *Trends Anal. Chem.* **2010**, *29*, 1004−1013. (c) Wencel, D.; Abel, T.; McDonagh, C. Optical chemical pH sensors. *Anal. Chem.* **2014**, *86*, 15−29.

(8) (a) DeFronzo, M.; Gillies, R. J. Characterization of methylphosphonate as a $^{31}$P NMR pH indicator. *J. Biol. Chem.* **1987**, *262*, 11032–11037. (b) Bruynseels, K.; Gillis, N.; Van Hecke, P.; Vanstapel, F. Phosphonates as $^{31}$P-NMR markers of extra- and intracellular space and pH in perfused rat liver. *NMR Biomed.* **1997**, *10*, 263–270. (c) Eykyn, T. R.; Kuchel, P. W. Scalar couplings as pH probes in compartimentalized biological systems: $^{31}$P NMR of phosphite. *Magn. Reson. Med.* **2003**, *50*, 693–696.

(9) (a) Pietri, S.; Miollan, M.; Martel, S.; Le Moigne, F.; Blaive, B.; Culcasi, M. α- and β-phosphorylated amines and pyrrolidines, a new class of low toxic highly sensitive $^{31}$P NMR pH indicators. Modeling of $pK_a$ and chemical shift values as a function of substituents. *J. Biol. Chem*. **2000**, *275*, 19505−19512. (b) Martel, S.; Clément, J. L.; Muller, A.; Culcasi, M.; Pietri, S. Synthesis and $^{31}$P NMR characterization of new low toxic highly sensitive pH probes designed for in vivo acidic pH studies. *Bioorg. Med. Chem*. **2002**, *10*, 1451−1458. (c) Culcasi, M.; Casano, G.; Lucchesi, C.; Mercier, A.; Clément, J. L.; Pique, V.; Michelet, L.; Krieger-Liszkay, A.; Robin, M.; Pietri, S. Synthesis and

biological characterization of new aminophosphonates for mitochondrial pH determination by $^{31}$P NMR spectroscopy. *J.Med. Chem*. **2013**, *56*, 2487−2499.

(10) (a) Pietri, S.; Martel, S; Culcasi, M.; Delmas-Beauvieux, M. C.; Canioni, P.; Gallis, J. L. Use of diethyl(2-methylpyrrolidin-2-yl)phosphonate as a highly sensitive extra- and intracellular $^{31}$P NMR pH indicator in isolated organs. Direct NMR evidence of acidic compartments in the ischemic and reperfused rat liver. *J. Biol. Chem*. **2001**, *276*, 1750−1758. (b) Gosset, G.; Satre, M.; Blaive, B.; Clément, J. L.; Martin, J. B.; Culcasi, M.; Pietri, S. Investigation of subcellular acidic compartments using α-aminophosphonate $^{31}$P nuclear magnetic resonance probes. *Anal. Biochem*. **2008**, *380*, 184−194. (c) Culcasi, M.; Thétiot-Laurent, S.; Atteia, A.; Pietri, S. Synthesis and biological characterization of new aminophosphonates for mitochondrial pH determination by $^{31}$P NMR spectroscopy. *Methods Mol. Biol.* **2015**, *1265*, 135−147.

(11) (a) Khramtsov, V. V.; Marsh, D.; Weiner, L.; Reznikov, V. A. The application of pH-sensitive spin labels to studies of surface potential and polarity of phospholipid membranes and proteins. *Biochim. Biophys. Acta* **1992**, *1104*, 317−324. (b) Reznikov, V. A.; Skuridin, N. G.; Khromovskikh, E. L.; Khramtsov, V. V. A new series of lipophilic pH-sensitive spin probes. *Russ. Chem. Bull., Int. Ed.* **2003**, *52*, 2052−2056. (c) Kirilyuk, I. A.; Bobko, A. A.; Grigor'ev, I. A.; Khramtsov, V. V. Synthesis of the tetraethyl substituted pH-sensitive nitroxides of imidazole series with enhanced stability towards reduction. *Org. Biomol. Chem.* **2004**, *2*, 1025−1030.

(12) (a) Khramtsov, V. V.; Weiner, L. M.; Eremenko, S. I.; Belchenko, O. I.; Schastnev, P. V.; Grigor'ev, I. A.; Reznikov, V. A. Proton exchange in stable nitroxyl radicals of the imidazoline and imidazolidine series. *J. Magn. Reson.* **1985**, *61*, 397−408. (b) Reznikov, V. A.; Skuridin, N. G.; Khromovskikh, E. L.; Khramtsov, V. V. A new series of lipophilic pH-sensitive spin probes. *Russ. Chem. Bull., Int. Ed.* **2003**, *52*, 2052−2056.

(13) (a) Gallez, B.; Mäder, K.; Swartz, H. M. Noninvasive measurement of the pH inside the gut by using pH-sensitive nitroxides. An in vivo study. *Magn. Reson. Med.* **1996**, *36*, 694−697. (b) Potapenko, D. I.; Foster, M. A.; Lurie, D.J.; Kirilyuk, I. A.; Hutchinson, J. M. S.; Grigor'ev, I.A.; Bagryanska, E. G.; Khramtsov, V.V. Real-time monitoring of drug-induced changes in the stomach acidity of living rats using improved pH-sensitive nitroxides and low-field EPR techniques. *J. Magn. Res*. **2006**, *182*, 1−11.

(14) Dembkovski, L.; Finet, J. P.; Fréjaville, C.; Le Moigne, F.; Maurin, R.; Mercier, A.; Pages, P.; Stipa, P.; Tordo, P. β-Phosphorylated five membered ring nitroxides. Synthesis and EPR study. Free Radic. Res. Commun. 1993, 19, S23-S32.

(15) (a) Haire, D. L.; Janzen, E. G.; Chen, G.; Robinson, V. J.; Hrvoic, I. New, stable β-phosphorus-labelled pyrrolidine nitroxides for magnetometry: an ESR investigation. *Magn. Reson. Chem.* **1999**, *37*, 251−258. (b) Clément, J. L.; Barbati, S.; Fréjaville, C.; Rockenbauer, A.; Tordo, P. Synthesis and use as spin trap of 5-methyl-5-phosphono-1-pyrroline *N*-oxide (DHPMPO). pH Dependence of the EPR parameters of the spin adducts. *J. Chem. Soc., Perkin Trans. 2*, **2001**, 1471−1475.

(16) (a) Grimaldi, S.; Finet, J. P.; Le Moigne, F.; Zeghdaoui, A.; Tordo, P.; Benoit, D.; Fontanille, M.; Gnagou, Y. Acyclic β-phosphorylated nitroxides: a new series of counter-radicals for "living"/controlled free radical polymerization. *Macromolecules* **2000**, *33*, 1141−1147. (b) Acerbis, S.; Bertin, D.; Boutevin, B.; Gigmes, D.; Lacroix-Desmazes, P.; Le Mercier, C.; Lutz, J. F.; Marque, S. R. A.; Siri, D.; Tordo, P. Intramolecular hydrogen bonding: The case of β-phosphorylated nitroxide (= aminoxyl) radical. *Helv. Chim. Acta* **2006**, *89*, 2119−2132.

(17) Audran, G.; Bosco, L.; Nkolo, P.; Bikanga, R.; Brémond, P.; Butscher, T.; Marque, S. R. A. The β-phosphorus hyperfine coupling constant in nitroxides: 6. Solvent effects in non-cyclic nitroxides. *Org. Biomol. Chem.* **2016**, *14*, 3729−3743.

(18) Amar, M.; Bar, S.; Iron, M. A.; Toledo, H.; Tumanskii, B.; Shimon, L. J. W.; Botoshansky, M.; Fridman, N.; Szpilman, A. M. Design concept for α-hydrogen-substituted nitroxides. *Nat. Commun.* **2015**, *6*, 6070.

(19) Matveeva, E. D.; Podrugina, T. A.; Prisyazhnoi, M. V.; Rusetskaya I. N.; Zefirov, N. S. Three component catalytic method for synthesis of α-amino phosphonates with the use of α-amino acids as amine components. *Russ. Chem. Bull., Int. Ed.* **2007**, *56*, 798−805.

(20) Bhowmick, M.; Sappidi, R. R.; Fields, G. B.; Lepore, S. D. Efficient synthesis of Fmoc-protected phosphinic pseudodipeptides: building blocks for synthesis of matrix metalloproteinase inhibitors. *Biopolymers* **2011**, *96*, 1−3.

(21) Spero, D. M.; Kapadia, S. R. Enantioselective synthesis of α-α-disubstituted amino acid derivatives via enzymatic resolution: prreparation of a thiazolyl-substituted α-methyl α-benzyl amine. *J. Org. Chem.* **1996**, *61*, 7398−7401.

(22) Moon, R. B.; Richards, J. H. Determination of intracellular pH by 31P magnetic resonance. *J. Biol. Chem.* **1973**, *248*, 7276–7278.

(23) Heller, C., McConnell, H. M. Radiation damage in organic crystals. II Electron spin resonance of $(CO_2H)CH_2CH(CO_2H)$ in β-succinic acid. *J. Chem. Phys.* **1960**, *32*, 1535−1540.

(24) Rockenbauer, A.; Györ, M.; Hankovszky, H. O.; Hideg, K. E.S.R. of the conformation of 5- and 6-membered cyclic nitroxide (aminoxyl) radicals. *Electron Spin Resonance* **1988**, *11A*, 145−182.

(25) Tordo, P.; Boyer, M.; Friedmann, A.; Santero, O.; Pujol, L. Phosphorus-substituted nitroxides. 3. Hyperconjugative ability of carbon-phosphorus bonds in five-membered ring nitroxides. *J. Phys. Chem.* **1978**, *82*, 1742−1744.

(26) Rockenbauer, A.; Szabo-Planka, T.; Arkosi, Z; Korecz, L. A two-dimensonal (magnetic field and concentration) electron paramagnetic resonance method for analysis of multispecies complex equilibrium systems. Information content of EPR spectra. *J. Am. Chem. Soc.* **2001**, *123*, 7646−7654.

(27) Saracino, G. A. A.; Tedeschi, A.; D'Errico, G.; Improta, R.; Franco, L.; Ruzzi, M.; Corvaia, C.; Barone, V. Solvent polarity and pH effects on the magnetic properties of ionizable nitroxide radicals: a combined computational and experimental study of 2,2,5,5-tetramethyl-3-carboxypyrrolidine and 2,2,6,6-tetramethyl-4-carboxypiperidine nitroxides. *J. Phys. Chem. A* **2002**, *106*, 10700−10706.

(28) Keana, J. F. W.; Pou, S.; Rosen, G. M. Nitroxides as potential contrast enhancing agents for MRI application: influence of structure onthe rate of reduction by rat hepatocytes, whole liver homogenate, subcellular fractions, and ascorbate. *Magn. Reson. Med.* **1987**, *5*, 525−536.

(29) (a) Mathieu, C.; Mercier, A.; Witt, D.; Debmkowski, L.; Tordo, P. β-Phosphorylated nitroxides in the pyrrolidine series: reduction by ascorbate. *Free Radic. Biol. Med.* **1997**, *22*, 803−906. (b) Jagtap, A. P.; Krstic, I.; Kunjir, N. C.; Hänsel, R.; Prisner, T. F.; Sigurdsson, S. T. Sterically shielded spin labels for in-cell EPR spectroscopy: analysis of stability in reducing environment. *Free Radic. Res.* **2015**, *49*, 78−85. (c) Kirilyuk, I. A.; Bobko, A. A.; Semenov, S. V.; Komarov, D. A.; Irtegova, I. G.; Grigor'ev, I. A.; Bagryanskaya, E. Effect of sterical shielding on the redox properties of imidazoline and imidazolidine nitroxides. *J. Org. Chem.* **2015**, *80*, 9118−9125.

(30) Cassien, M.; Petrocchi, C.; Thétiot-Laurent, S.; Robin, M.; Ricquebourg, E.; Kandouli, C.; Asteian, A.; Rockenbauer, A.; Mercier, A.; Culcasi, M.; Pietri, S. On the vasoprotective mechanisms underlying novel ß-phosphorylated nitrones: focus on free radical characterization, scavenging and NO-donation in a biological model of oxidative stress. *Eur. J. Med. Chem.* **2016**, *119*, 197−217.

(31) Pietri, S.; Mercier, A.; Mathieu, C.; Caffaratti, S.; Culcasi, M. Hemodynamic and metabolic effects of the β-phosphorylated nitroxide 2-diethoxyphosphoryl-2,5,5-trimethylpyrrolidinoxyl during myocardial ischemia and reperfusion. *Free Radic. Biol. Med.* **2003**, *34*, 1167−1177.

(32) Pietri, S.; Liebgott, T.; Fréjaville, C.; Tordo, P.; Culcasi, M. Nitrone spin traps and their pyrrolidine analogs in myocardial reperfusion injury: hemodynamic and ESR implications. Evidence for a cardioprotective phosphonate effect for 5-(diethoxyphosphoryl)-5-methyl-1-pyrroline *N*-oxide in rat hearts. *Eur. J. Biochem.* **1998**, *254*, 256−265.

(33) Cianci, J.; Baell, J. B.; Harvey, A. J. Microwave-assisted, zinc-mediated peptide coupling of *N*-benzyl-α,α-disubstituted amino acids. *Tetrahedron Lett.* **2007**, *48*, 5973−5975.

(34) Hess, B.; Kutzner, C.; van der Spoel, D.; Lindahl, E. GROMACS 4: Algorithms for highly efficient, load-balanced, and scalable molecular simulation. *J. Chem. Theory Comput.* **2008**, *4*, 435−447.

(35) Frisch, M. J.; Trucks, G. W.; Schlegel, H. B.; Scuseria, G. E.; Robb, M. A.; Cheeseman, J. R.; Scalmani, G.; Barone, V.; Mennucci, B.; Petersson, G. A.; Nakatsuji, H.; Caricato, M.; Li, X.; Hratchian, H. P.; Izmaylov, A. F.; Bloino, J.; Zheng, G.; Sonnenberg, J. L.; Hada, M.; Ehara, M.; Toyota, K.; Fukuda, R.; Hasegawa, J.; Ishida, M.; Nakajima, T.; Honda, Y.; Kitao, O.; Nakai, H.; Vreven, T.; Montgomery, J. A., Jr.; Peralta, J. E.; Ogliaro, F.; Bearpark, M.; Heyd, J. J.; Brothers, E.; Kudin, K. N.; Staroverov, V. N.; Kobayashi, R.; Normand, J.; Raghavachari, K.; Rendell, A.; Burant, J. C.; Iyengar, S. S.; Tomasi, J.; Cossi, M.; Rega, N.; Millam, J. M.; Klene, M.; Knox, J. E.; Cross, J. B.; Bakken, V.; Adamo, C.; Jaramillo, J.; Gomperts, R.; Stratmann, R. E.; Yazyev, O.; Austin, A. J.; Cammi, R.; Pomelli, C.; Ochterski, J. W.; Martin, R. L.; Morokuma, K.; Zakrzewski, V. G.; Voth, G. A.; Salvador, P.; Dannenberg, J. J.; Dapprich, S.; Daniels, A. D.; Farkas, O.; Foresman, J. B.; Ortiz, J. V.; Cioslowski, J.; Fox, D. J. Gaussian, Inc.: Wallingford CT, **2009**.

(36) Jorgensen, W. L.; Madura, J. D. Quantum and statistical mechanical studies of liquids. 25. Solvation and conformation of methanol in water. *J. Am. Chem. Soc.* **1983**, *105*, 1407−1473.

(37) Hornak, V.; Abel, R.; Okur, A.; Strockbine, B.; Roitberg, A.; Simmerling, C. Comparison of multiple Amber force fields and development of improved protein backbone parameters. *Proteins: Struct., Funct., Bioinf.* **2006**, *65*, 712−725.

(38) Stendardo, E.; Pedone, A.; Cimino, P.; Menziani, M. C.; Crescenzi, O. ; Barone, V. Extension of the AMBER force-field for the study of large nitroxides in condensed phases: an ab initio parameterization. *Phys. Chem. Chem. Phys.* **2010**, *12*, 11697−11709.

(39) Wang, J.; Cieplak, P.; Kollman, P. A. How well does a restrained electrostatic potential (RESP) model perform in calculating conformational energies of organic and biological molecules? *J. Comput. Chem.* **2000**, *21*, 1049-1074.

(40) Rockenbauer, A.; Korecz, L. Automatic computer simulations of ESR spectra. *Appl. Magn. Reson.* **1996**, *10***,** 29-43.

(41) Flecknell, P. A.; Roughan, J. V.; Hedenqvist, P. Induction of anaesthesia with sevoflurane and isoflurane in the rabbit. *Lab. Anim*. **1999**, *33*, 41−46.

**Table 1.** $^{31}$P NMR pH Calibration[a] and Relaxation[b] Characteristics of α-Aminophosphonates Esters in Biologically Relevant Media[c]

| compd | medium | p$K_a$ | $\delta_a$ | $\delta_b$ | $\Delta\delta_{ab}$ | $T_1$ |
|---|---|---|---|---|---|---|
| | | | (ppm) | | | (s) |
| $P_i$ | KH | 6.64 | 0.68 | 3.26 | 2.58 | 9.80−11.50 |
| | $CytM_h$ | 6.78 | 0.68 | 3.22 | 2.54 | 1.30−3.80 |
| **3a** | KH | 3.63 | 22.31 | 32.69 | 10.38 | 3.60 |
| 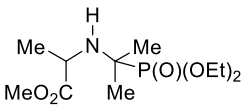 | $CytM_h$ | 3.48 | 22.48 | 32.84 | 10.36 | 2.97 |
| | $CytM_l$ | 3.52 | 22.48 | 32.71 | 10.23 | 2.41 |
| **3b** | KH | 3.35 | 22.29 | 32.68 | 10.39 | 2.90 |
| 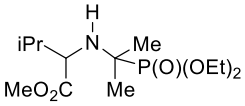 | PB | 3.24 | 21.81 | 32.21 | 10.40 | 3.00 |
| **3c** | KH | 2.60 | 22.15 | 32.52 | 10.37 | 2.40 |
| 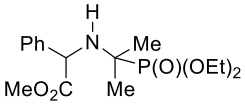 | $CytM_h$ | 2.48 | 22.34 | 32.41 | 10.04 | nd[d] |
| **9a** | KH | 2.39 | 20.20 | 30.74 | 10.54 | 3.07 |
| 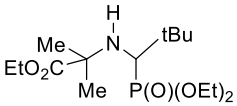 | $CytM_l$ | 2.47 | 20.81 | 30.62 | 9.81 | 0.30 |
| | PB | 2.54 | 20.63 | 30.09 | 9.46 | 1.91 |
| **9b** | KH | 2.99 | 19.73 | 29.91 | 10.18 | 3.20 |
| 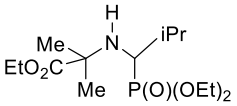 | $CytM_l$ | 2.95 | 19.89 | 29.80 | 9.91 | 1.55 |
| | PB | 3.18 | 19.47 | 29.27 | 9.80 | 5.58 |
| (2*S*,1'*S*)-**16** | PB | nd | 27.76 | 27.74 | 0.02 | 6.83[e] |
| 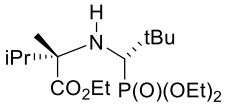 | | | | | | |

Table 1 (continued)

| | | | | | | |
|---|---|---|---|---|---|---|
| (2*S*,1'*R*)-**16** | PB | nd | 30.61 | 30.61 | 0 | 6.15[e] |

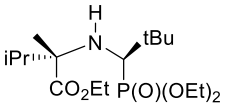


---

[a] $\delta_a$ and $\delta_b$, limiting chemical shift of the protonated and unprotonated form, respectively; $\Delta\delta_{ab} = \delta_a - \delta_b$; determined at 22 °C and given as means from 3−10 repeated titrations with < 1% precision. [b] $T_1$ = longitudinal relaxation time measured at pH ≈ p$K_a$. [c] $P_i$, inorganic phosphate; KH, Krebs-Henseleit medium; $CytM_h$, rat heart cytosolic homogenate; $CytM_l$, rat liver cytosolic homogenate; PB, phosphate buffer (i.e., 1 mM $KH_2PO_4$). [d] not determined. [e] pH 4.00.

**Table 2.** Selected Crystallographic data of **10b** (R = Me) and Molecular Dynamics Simulation for the Average Geometry of the (*S*) Enantiomer of **10b**, **11b** (R = H), **5a** (R' = Me) and **5c** (R' = Ph) in Aqueous Solution.[a]

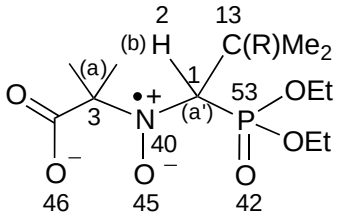


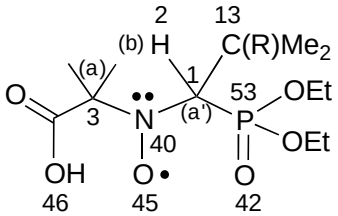


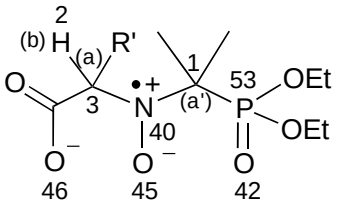


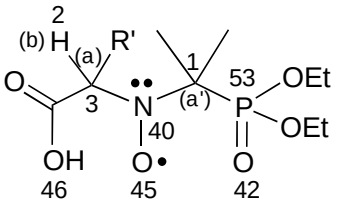


| | X-ray | unprotonated | | protonated | | unprotonated | | protonated | |
|---|---|---|---|---|---|---|---|---|---|
| compd | **10b** | **10b** | **11b** | **10b** | **11b** | **5a** | **5c** | **5a** | **5c** |
| Bond lengths (Å) | | | | | | | | | |
| C(1)−P(53) | 1.835(2) | 1.84(3) | 1.83(3) | 1.83(3) | 1.82(3) | 1.83(3) | 1.83(3) | 1.83(3) | 1.83(3) |
| C(1)−C(13) | 1.569(3) | 1.57(3) | 1.56(3) | 1.57(3) | 1.56(3) | —— | —— | —— | —— |
| N(40)−C(1) | 1.473(3) | 1.50(3) | 1.50(3) | 1.50(3) | 1.50(3) | 1.50(3) | 1.51(3) | 1.51(3) | 1.51(3) |
| N(40)−O(45) | 1.288(2) | 1.27(3) | 1.27(3) | 1.27(3) | 1.27(3) | 1.27(3) | 1.27(3) | 1.27(3) | 1.27(3) |
| N(40)−C(3) | 1.482(3) | 1.50(3) | 1.51(3) | 1.51(3) | 1.51(3) | 1.50(3) | 1.49(3) | 1.50(3) | 1.50(3) |
| Distances (Å) | | | | | | | | | |
| O(42).....N(40) | 3.124 | 3.7(3) | 3.6(4) | 3.7(3) | 3.6(3) | 3.5(4) | 3.6(4) | 3.6(3) | 3.6(4) |
| O(46).....N(40) | 2.683 | 3.2(2) | 3.2(2) | 3.2(2) | 3.2(2) | 3.2(2) | 3.2(3) | 3.2(2) | 3.0(2) |
| Bond angle (°) | | | | | | | | | |
| C(3)−N(40)−C(1) | 126.77(19) | 126(3) | 126(3) | 126(3) | 126(3) | 125(3) | 124(3) | 125(3) | 125(3) |

Table 2 (continued)

| | | | | | | | | | |
|---|---|---|---|---|---|---|---|---|---|
| Dihedral angles (°) | | | | | | | | | |
| P(53)−C(1)−N(40)−O(45) | −76.47 | −70(11) | −70(11) | −70(12) | −71(12) | 96(30) | 99(25) | −93(34) | −106(34) |
| | | | | | | | | 93(35)[b] | 97(32)[b] |
| H(2)−C(1)−N(40)−O(45) | 170.90 | −179(12) | 177(12) | 179(12) | 175(12) | −174(17) | −171(25) | 179(17) | 179(25) |

[a]Values in parentheses are the estimated SD. In all structures atom numbering is given similar to the deposited structure of **10b**. [b]Values obtained for alternative stable conformations.

**Table 3.** Calculated EPR Parameters of β-Diethoxyphosphoryl Nitroxides at 22 °C

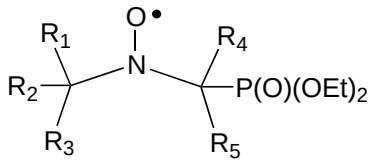


| compd | medium[a] | $R_1$ | $R_2$ | $R_3$ | $R_4$ | $R_5$ | $a_N$ (G) | $a_{H\beta}$ (G) | $a_P$ (G) | long-range couplings (G) | *g* |
|---|---|---|---|---|---|---|---|---|---|---|---|
| **5a** | PB (pH 6.62) | H | Me | $CO_2^-$ | Me | Me | 14.62 | 4.88 | 51.45 | 0.27(3H), 0.15(3H) | —— |
| **5c** | PB (pH 6.25) | H | Ph | $CO_2^-$ | Me | Me | 14.50 | 4.48 | 49.47 | 0.35(3H) | —— |
| **10a** | W (pH 7.12) | Me | Me | $CO_2Et$ | H | *t*-Bu | 14.38 | 1.29 | 41.75 | 0.45(3H), 0.26(3H) | 2.00557 |
| **10b** | W (pH 6.56) | Me | Me | $CO_2^-$ | H | *t*-Bu | 14.67 | 1.43 | 40.25 | 0.36(3H), 0.26(3H), 0.23(9H) 5.6($2\times^{13}C$), 7.4($3\times^{13}C$) | 2.00547 |
| **11b** | PB (pH 6.67) | Me | Me | $CO_2^-$ | H | i-Pr | 14.92 | 1.39 | 44.04 | 0.45(3H), 0.22 (6H), 0.10(1H) | 2.00636 |
| **12** | W (pH 3.23) | Me | Me | $CO_2Et$ | H | *i*-Pr | 14.59 | 1.38 | 44.05 | 0.39(3H), 0.21(6H) | 2.00543 |
| (2*S*,1'*S*)-**17** | W (pH 7.17) | Me | *i*-Pr | $CO_2Et$ | H | *t*-Bu | 13.69 | 1.17 | 38.46 | 0.30(1H) | 2.00560 |
| (2*S*,1'*R*)-**17** | W (pH 7.08) | Me | *i*-Pr | $CO_2Et$ | H | *t*-Bu | 14.65 | 1.47 | 43.61 | 3.95(1H) | 2.00554 |
| DEPN | PB (pH 7.3) | Me | Me | Me | H | *t*-Bu | 14.93 | 0.99 | 45.68 | 0.34(9H) | 2.00542 |

[a]W, water; PB, 20 mM phosphate buffer.

**Table 4.** EPR pH-Calibration Parameters of β-Phosphorylated Carboxylic Nitroxides at 22 °C[a]

| compd | medium[b] | limiting hyperfine splittings (G)[c] and p$K_a$ values | | | | | | | | | |
|---|---|---|---|---|---|---|---|---|---|---|---|
| | | from $a_N$ titration curve | | | from $a_H$ titration curve | | | from $a_P$ titration curve | | | 2-D[d] |
| | | $(a_N)_a$ | $(a_N)_b$ | p$K_a$ | $(a_H)_a$ | $(a_H)_b$ | p$K_a$ | $(a_P)_a$ | $(a_P)_b$ | p$K_a$ | p$K_a$ |
| **5a** | | | | | | | | | | | |
| | PB | 14.49 ± 0.02 | 14.67 ± 0.01 | 2.91 ± 0.06 | 2.53 ± 0.04 | 4.88 ± 0.01 | 2.97 ± 0.02 | 47.71 ± 0.04 | 51.45 ± 0.01 | 2.95 ± 0.01 | 2.57 |
| | $CytM_h$ | 14.48 ± 0.04 | 14.67 ± 0.04 | 3.11 ± 0.04 | 2.47 ± 0.03 | 4.93 ± 0.09 | 3.06 ± 0.01 | 47.67 ± 0.03 | 51.56 ± 0.01 | 3.06 ± 0.01 | |
| **5c** | | | | | | | | | | | |
| | PB | 14.25 ± 0.01 | 14.50 ± 0.01 | 2.47 ± 0.06 | 2.69 ± 0.02 | 4.50 ± 0.01 | 2.48 ± 0.02 | 45.67 ± 0.06 | 49.55 ± 0.03 | 2.45 ± 0.02 | 2.49 |
| | $CytM_h$ | 14.26 ± 0.01 | 14.50 ± 0.01 | 2.54 ± 0.07 | 2.74 ± 0.02 | 4.46 ± 0.01 | 2.50 ± 0.02 | 45.77 ± 0.09 | 49.45 ± 0.03 | 2.51 ± 0.02 | |
| **10b** | | | | | | | | | | | |
| | PB | 14.34 ± 0.01 | 14.67 ± 0.01 | 3.61 ± 0.03 | 1.28 ± 0.01 | 1.42 ± 0.01 | 3.59 ± 0.07 | 42.10 ± 0.02 | 40.23 ± 0.01 | 3.60 ± 0.03 | 3.76 |
| | $CytM_l$ | 14.32 ± 0.01 | 14.66 ± 0.01 | 3.58 ± 0.02 | 1.27 ± 0.01 | 1.42 ± 0.01 | 3.44 ± 0.02 | 42.05 ± 0.02 | 40.21 ± 0.01 | 3.59 ± 0.02 | |
| | $CytM_s$ | 14.32 ± 0.01 | 14.70 ± 0.01 | 3.56 ± 0.02 | 1.27 ± 0.01 | 1.42 ± 0.01 | 3.52 ± 0.01 | 42.05 ± 0.02 | 40.22 ± 0.01 | 3.58 ± 0.02 | |
| **11b** | | | | | | | | | | | |
| | PB | 14.56 ± 0.01 | 14.91 ± 0.01 | 3.41 ± 0.02 | 1.37 ± 0.01 | 1.39 ± 0.01 | 3.59 ± 0.29 | 44.36 ± 0.01 | 44.00 ± 0.01 | 3.35 ± 0.06 | 3.62 |

Table 4 (continued)

[a]Mean ± SD ($n$ = 2−4 independent titrations). [b]PB, 20 mM phosphate buffer; $CytM_h$, rat heart cytosolic homogenate; $CytM_l$, rat liver cytosolic homogenate; $CytM_s$, rat stomach cytosolic medium. [c]$(a_X)_a$, limiting coupling constant in the protonated form; $(a_X)_b$, limiting coupling constant in the unprotonated form. [d]Two-dimensional EPR simulation.

**Table 5.** Cytotoxicity of β-Phosphorylated Nitroxides and Amines pH Markers against A549 Cells and Normal Human Lung Fibroblasts (NHLF)[a], and Predicted Lipophilicities.

| compd | $IC_{50}$ (mM)[b] | | | | | | AlogP[c] |
|---|---|---|---|---|---|---|---|
| | FMCA | | MTT | | LDH | | |
| | A549 | NHLF | A549 | NHLF | A549 | NHLF | |
| DEPN | 4.4 ± 0.2 | nd[d] | 2.5 ± 0.1 | nd | 4.2 ± 0.3 | nd | 2.01 |
| TMPPO | 12.1 ± 2.1 | 19.8 ± 2.4 | 10.5 ± 2.4 | 17.5 ± 0.9 | > 45 | 40.8 ± 2.4 | 1.12 |
| **10b** | 15.8 ± 1.4 | 13.8 ± 0.4 | 13.2 ± 1.6 | 10.3 ± 0.9 | 13.5 ± 2.0 | 9.2 ± 1.3 | 1.71 |
| **3a** | 18.4 ± 1.6 | 10.8 ± 1.2 | 22.7 ± 1.2 | 13.8 ± 1.2 | 25.3 ± 1.9 | 12.5 ± 1.0 | 1.68 |
| **3b** | 12.7 ± 0.4 | 2.2 ± 0.5 | 6.7 ± 1.2 | 3.5 ± 0.3 | 12.4 ± 1.5 | 8.1 ± 0.2 | 2.27 |
| **3c** | 1.7 ± 0.4 | 1.8 ± 0.1 | 1.8 ± 0.2 | 1.0 ± 0.2 | 2.1 ± 0.2 | 1.1 ± 0.1 | 2.71 |
| **9a** | 3.9 ± 0.5 | 1.4 ± 0.3 | 4.9 ± 0.3 | 1.5 ± 0.1 | 5.1 ± 0.4 | 4.1 ± 0.1 | 2.21 |
| **9b** | 7.6 ± 0.1 | 3.4 ± 1.3 | 14.3 ± 0.2 | 4.2 ± 1.4 | 19.8 ± 0.2 | 3.8 ± 0.9 | 1.88 |
| DEPMPH | 70.2 ± 2.1 | 62.5 ± 0.8 | 72.5 ± 0.9 | 60.9 ± 1.1 | 126.3 ± 1.5 | 102.2 ± 1.2 | 1.04 |

[a]Cells seeded at $2.5 \times 10^4$ cells/well in DMEM (A549) or FBM (NHLF) until confluence were treated with test compounds at 0.01−100 mM for 48 h. Data are means ± SD of 3−6 independent experiments made in triplicate for at least four concentrations. [b]$IC_{50}$ defined as the concentration of compound resulting in 50% cell viability (FMCA and MTT; calculated from concentration-response curves) or 50% decrease of intracellular LDH content with respect to total LDH. [c]Obtained using the ALOGPS 2.1 software (www.vcclab.org/lab/alogps/). [d]not determined.